

1

Spheres, Clusters and Packing of Spheres

1.1

Introduction

Imagine, Design, Create, Explore

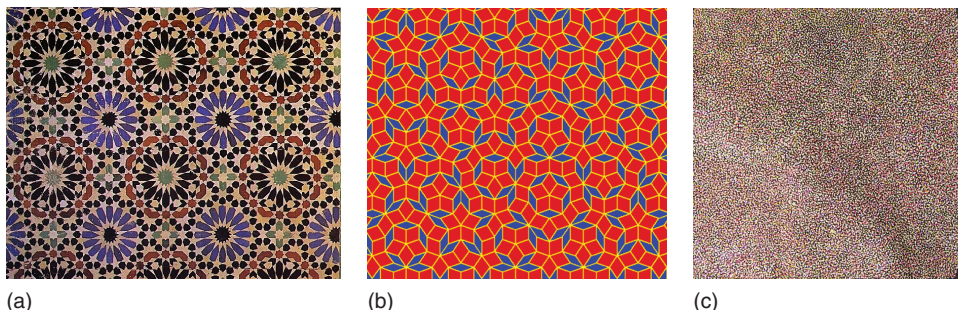
Theory of amorphousness is a science about the structural arrangement of atoms in amorphous solids. It is part of Materials Science, which includes the closely related theory of crystallography. Whilst theory of crystallography is well established, theory of amorphousness is beginning to emerge as a body of science in its own right.

Arrangement of objects leads to creation of patterns. The invention of a repeating pattern as a thoughtful and creative process has ancient beginnings, at first in art as discovered by archaeology and evidenced in mosaics existing in ancient buildings, and later in science as known from old manuscripts; for example the five ideal Greek solids. There are three types of patterns that can fill in Euclidean space contiguously, and to infinity. These are:

- patterns with translational symmetry that possess an underlying lattice
- patterns with fivefold rotational symmetry but without translational symmetry
- random patterns with no lattice and no rotational symmetry.

Two-dimensional examples of such patterns are shown in Figure 1.1. All three are used as conceptual models for atomic arrangements in solids.

Crystalline solids have been known and appreciated since antiquity. In modern times the intrinsic elements of symmetry in single crystals of minerals were given attention in 1822 by R. J. Haüy (pronounced \bar{a} -wee, \bar{a} as in ‘aside’) in ‘*Traité de Cristallographie*’. Shortly after, the theoretical treatments of W. H. Miller in 1839 on hkl notation, A. Bravais in 1845 on 14 lattices, A. Schönflies in 1892 and W. Barlow in 1898 on 230 space groups (with many contributions from others) resulted in a complete theory of geometrical crystallography. Perfectly regular and ordered structures of infinite extent are described by geometrical crystallography as perfect (*ideal*) solids, with positions and arrangements of all atoms defined precisely along specific lattices. Theory of crystallography provides a datum from which the ideal atomic arrangements (and defects) in real materials can be determined. By comparison, no such universal laws or rules are well known for the atomic structure in amorphous solids.



(a)

(b)

(c)

Figure 1.1 (a-c) Fragments of two-dimensional patterns representing the three formats of atomic arrangement in solids: crystalline (tiles from Morocco),

quasi-crystalline (computer pattern generated by T.R. Welberry of ANU) and amorphous (Aboriginal painting by Ada Ross, Australia).

In a historical perspective, it would be interesting to contemplate the following question: if Pythagoras were a statistician rather than deducing perfect harmony from ratios of pure numbers on strings, would we have had a theory of amorphousness in solid-state developed ages ago? Looking back in time, one can draw a direct line from the modern theory of geometric crystallography to the philosophy of pure numbers and rational ratios of antiquity. The René-Just Haüy description of packing of elementary blocks to form a single crystal with a simple relationship between its crystal faces and packing arrangement derives directly from the deductive Pythagorean notion of perfect harmony based on the relationship between the length of the string and perfect harmonic notes as 1 : 2, 2 : 3, 3 : 4, and so on. The relationship between atomic planes and crystal lattice is also expressed by simple ratios of whole numbers, the reciprocals of which are known as *Miller indices*. By comparison, relatively little is known about the structure of amorphous solids. Our knowledge of amorphous structures seems incomplete when compared with that of crystalline solids. In particular, the concept of an ideal amorphous solid as a datum and the corresponding theory have been lacking hitherto.

Until quite recently, amorphous solids were described as disordered crystalline solids, with some degree of order intermediate between a liquid and a solid. This was based on the understanding that glasses are free from the constraints that govern the arrangements of atomic clusters in crystalline materials, so there is a degree of ambiguity in the way that neighbouring clusters can be positioned and oriented.

A possible implication deriving from this view is that amorphous solids originate from the corresponding ordered crystalline state. In the field of geometric crystallography, a disordered crystalline structure implies the presence of defects which are defined relative to the perfectly ordered structure. Therefore, disordered materials are crystalline materials that, in principle, can be restored to the perfect crystalline state by the reversal of defects. It is conjectured that this cannot be done in amorphous materials and that a different approach and terminology



Figure 1.2 A view of the structure of solids along an undefined, somewhat arbitrary variable. The circles indicate the positions of the ideal (perfect) structures; the lines indicate the spectrum of structures in real solids.

should be used to describe their structure, namely, *random* atomic arrangement. To emphasize this point, we note that in the field of statistics, when describing a set of *random* data, it would be unfitting to refer to that set as *disordered* data. Hence, it is proposed that amorphous structures, based on irregular packing of spheres, should be referred to as having a random arrangement of atoms rather than a disordered atomic arrangement. To promote this view, a drawing is shown in Figure 1.2 with the contemplated relative positions of the two types of solids and the envisaged discontinuity between the random and ordered types of atomic arrangements that must exist. The very small gap between the circle and the line on the crystalline side indicates that almost perfect single crystals can be grown. The larger gap on the amorphous side indicates that the structure of glasses may not be as close to the ideal amorphous solid as described later in this book. A discontinuity in the line near the middle is meant to indicate that even highly disordered crystalline solids are not the same as highly flawed amorphous glasses, and vice versa. This view is very close to that expressed by Kazunobu Tanaka *et al.* in the introduction to their book on 'Amorphous Silicon'.

A scientifically satisfactory explanation of the amorphous state continues to be a challenge, and for this reason, we advance and promote the theoretical concept of an *ideal amorphous solid* as a partial solution to this enigma. The right approach to a definition of amorphousness is through an appropriate geometric and topological model of the ideal amorphous solid, as described in this chapter.

However, the usage of the word 'disordered' appears in dictionaries to mean unpredictable, opposite to law and order. So, this seems to be also a matter of habit and semantics, rather than a question of pure logic. Nevertheless, an appropriate and consistent vocabulary conjures up a clear vision of the atomic arrangements and helps to define the field of science of amorphous solids, separate and distinct from the field of crystallography.

The study of atomic arrangements in amorphous solids was stimulated in the 1960s by theoretical work of J. D. Bernal on the structure of liquids, concurrent with experimental random packing of spheres by G. D. Scott. In the last few decades, research into atomic arrangements in amorphous solids has separated into two main streams: (i) more refined and detailed studies of packing of spheres and molecules and (ii) atomistic simulations by molecular dynamics (MD), including *ab-initio* methods. The understandings we gain from the two approaches are of different nature. In the latter approach, a unique definition of an amorphous

atomic structure cannot be achieved because in a simulated thermodynamic system with suppressed self-assembly tendencies every simulation, even repeated on the same system, must result in a different atomic arrangement. Modelling amorphous materials by these methods is equivalent to random packing with extreme cooling rates of the order of 10^{15} K s $^{-1}$. Nevertheless, these methods are successful and appropriate to simulate the structure of real amorphous solids with atomic arrangements containing imperfections. In the former case, simulations and geometrical modelling follow the methodology of representing atoms by hard spheres and creating representations of random atomic arrangement, naturally quite different from crystalline structures.

The earliest concept of atoms appears in a written record from Leucippus of Miletus (once an ancient Greek city on the western coast of Anatolia) and Democritus of Abdera (city-state on the coast of Thrace, its foundation attributed to Heracles), Greek philosophers of 5–4th century BC (Taylor, 1999). They conjectured that as matter is divided into smaller and smaller parts, there must be a limit to this division; namely atoms, the smallest indivisible objects. Otherwise, if there were no limit to the division, then the parts could be divided into “nothingness”, and therefore, matter would not exist (*reductio ad absurdum* method of logic). Their theory envisaged atoms as invisible and indivisible particles, not as perfectly shaped as spheres but in the form of odd shapes with hooks and protrusions to render various properties of matter, such as taste, colour, fluidity and friction, as described by the Roman poet, Lucretius, in his *De Rerum Natura* (first century BC didactic poem on Epicurean philosophy). Coincidentally, modern view of atoms also shows electronic orbitals as having various shapes and protrusions, although the complete atom, encompassing all the orbitals, is imagined as having a spherical shape (Figure 1.3).

The concept of representing atoms by spheres has evolved gradually and over a long period of time. In 1611, Joannis Kepler drew hexagonal close packing of spheres to illustrate a compact solid (Kepler, 1611) and suggested that the hexagonal symmetry of snowflakes is due to the regular packing of the constituent particles. Some 50 years later, Robert Hooke wrote that crystals are composed of close packed ‘spheroids’. At that time it was thought that spherical atomic particles must be close packed to form a rigid solid. Layers of round spherical objects,

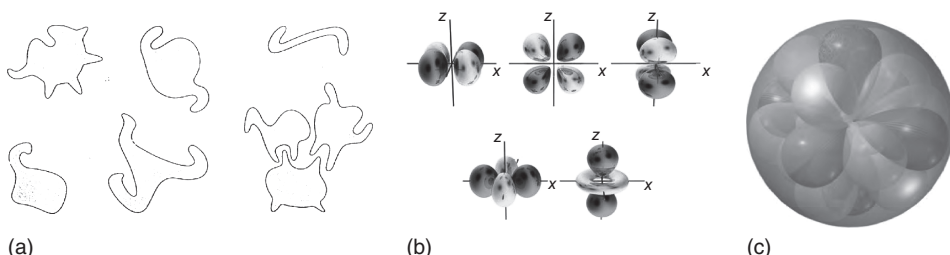


Figure 1.3 (a) Atoms of Leucippus and Democritus as depicted by Lucretius (Adapted from *Scientific American*). (b) Quantum mechanics view of electron clouds around atoms. (c) View of an atom as a sphere encompassing all electronic orbitals.

close packed in a hexagonal arrangement in repeating stacks of ABABAB... pattern, formed such an arrangement with fundamental sixfold symmetry, known in crystallography as hexagonal close packed (hcp). Soon, a variation of this layered packing was discovered, with a stacking sequence of ABCABC.., which gives a so-called face centred cubic (fcc) arrangement with characteristic fourfold and threefold symmetry.

The representation of atoms as spheres is not only intuitive, it is also in part justified by the Born–Oppenheimer approximation, which states that

$$\Psi_{\text{total}} = \psi_{\text{electronic}} \times \psi_{\text{nuclear}} \quad (1.1)$$

In simple terms, the approximation allows the wave function of a molecule, Ψ_{total} , to be separated into its electronic and nuclear components. The success of the BO approximation relies on the fact that spinning and oscillations of the electrons are several orders of magnitude higher than the frequency of oscillations of the nuclei. Consequently, the electrons surround the nuclei like clouds, on average spherically distributed around the central core. This is supported by many instances, for example, by the behaviour of colliding atoms which rebound in a way similar to that of billiard balls on a snooker table. In metals the electrons in the inner shells are strongly bound, and the electron density in the ionic core, which holds most of the electrons, satisfies the spherical distribution of electronic density, $\rho(\mathbf{r})$.

Early writing on mineralogy, especially on gemstones, comes from ancient Babylonia, the ancient Greco-Roman world, ancient and medieval China and Sanskrit texts from ancient India and the ancient Islamic World. Books on the subject include the *Naturalis Historia* of Pliny the Elder, and *Kitab al Jawahir* (Book of Precious Stones) by Muslim scientist Al Biruni. The German Renaissance specialist Georgius Agricola wrote works such as *De re metallica* (On Metals, 1556) and *De Natura Fossilium* (On the Nature of Rocks, 1546) which begin the scientific approach to the subject. Systematic scientific studies of minerals and rocks developed in post-Renaissance Europe. Figure 1.4 shows portraits of people who contributed to the early stages of crystallography.



Figure 1.4 Portraits by various artists: Joannis Kepler, Dutch astronomer (1571–1630), Robert Hooke, English natural philosopher (1635–1703), Niels Stensen, Danish geologist (1638–1686) and René Just Haüy, French mineralogist (1743–1822) reproduced from Wikipedia.

Steno gave the first accurate observations on a type of crystal in his 1669 book *De solido intra solidum naturaliter contento*. The principle in crystallography, known as *Steno's law of constant angles* or simply as *Steno's law*, states that the angles between corresponding faces on crystals are the same for all specimens of the same mineral. Steno's seminal work paved the way for the law of the rationality of the crystallographic indices of French mineralogist René-Just Haüy in 1801.

Mineralogy played an important role in the eighteenth century in establishing the principles of crystallography, in which crystals are represented by ordered packing of spheres in a unit cell. At the start of nineteenth century René-Just Haüy published a book on crystallography and substantiated the law of rational indices (Haüy, 1821), which later gave rise to Miller indices. In the book, single crystals were envisaged as ordered packing of spheres in regular polyhedra with angles between their faces corresponding precisely to the angles found in natural crystals. Hence, different arrangements resulted in different angles for different crystals—a glimpse into the nature of crystals.

Mineralogists and crystallographers focused on models of ideal solids with ordered, symmetrical arrangements, whereas mathematicians continued to ponder, amongst other things, about random, irregular packings, and physicists used the results to describe fluidity of liquids (Bernal, 1959), and now the atomic arrangements in amorphous materials.

Excerpt from:

"RENE-JUST HAÜY AND HIS INFLUENCE"

by HERBERT P. WHITLOCK

New York State Museum

Essai d'une théorie sur la structure des cristaux (1784)

Trait de cristallographie (1822, 2 vols.)

Volume 3, pages 92–98, 1918

We know that in the house of his friend, M. Defrance, Haüy dropped the now historic group of prismatic crystals of calcite and gathered from the ruin of a fine specimen the cleavage pieces to him recognizable as of the same form as other crystals of calcite; it thus appears that he had inevitably thrust upon him the key to the mystery of the mathematical inter-relation of these forms. But without a mind prepared to interpret this chance occurrence, without the imagination reaching out to its interpretation, the incident would have meant no more to him than to his friend who stood beside him. Bergmann, although unknown to Haüy, had an almost identical incident called to his attention by his pupil Gahn but had failed to fully realize its significance. Bergmann did not voice the cry, which on the lips of his illustrious successor has become historic, 'Tout est trouvé'.

Returning to his cabinet, Haüy lost no time in verifying the principle which was thus revealed to him. Under his hammer were sacrificed successively a scaleno-hedral crystal of calcite of the form known as *dog tooth spar* and another of a low rhombohedral habit; in each case, the primitive cleavage rhombohedron appeared

amongst the fragments, as he expected that it would. With the idea of developing the ‘primitive form’ from other species, he ruthlessly attacked the other treasured specimens of his little collection and his sacrifice was fully justified by the results, for the cleavage fragments in many instances furnished him with the basis, significantly termed by him *le noyau*, upon which the complicatedly modified crystal combinations were, as it were, built up. He conceived the theory of modified forms, built up from the primitive by diminishing layers of crystal particles (*décroisements*), each successive layer having a definite relation to the preceding one and primitive nucleus.

By the early nineteenth century, the size of atoms was estimated by chemists to be very small, deduced from the knowledge of one gramme-mole (Amedeo Avogadro, Italian savant (1776–1856)) and density (Archimedes (287–c.212 BC)). However, precise atomic dimensions were only determined with the application of X-rays to the diffraction from crystalline solids in the first decade of the twentieth century. In Bragg’s law, the distance between interatomic planes relates simply to the inverse of the angle of the diffracted beam, which allows for great accuracy of measurement of atomic dimensions. It turned out that atomic diameters are of the order of 10^{-10} m, and at that time, it was proposed to define a special unit of measure for that purpose, called *angstrom* Å, named after the Swedish physicist Anders Jonas Angström (1814–1874). For example, the atomic radius of phosphorus (P) is almost exactly 1 Å.

In the 1950s, Robert Corey and Linus Pauling at the California Institute of Technology created accurate scale models (1 inch = 1 Å) of molecules using hardwood spheres. Since then, textbooks on crystallography and materials science are ubiquitous in the use of spheres to represent atoms arranged in unit cells and on crystalline lattices. In chemistry, a space-filling model is a three-dimensional molecular model where the atoms are represented by spheres with sizes proportional to the radii of the atoms, as shown in Figure 1.5.

In mathematical geometry, the packing of hard (non-intersecting) spheres, both ordered and disordered, is a challenging subject with a long history. It

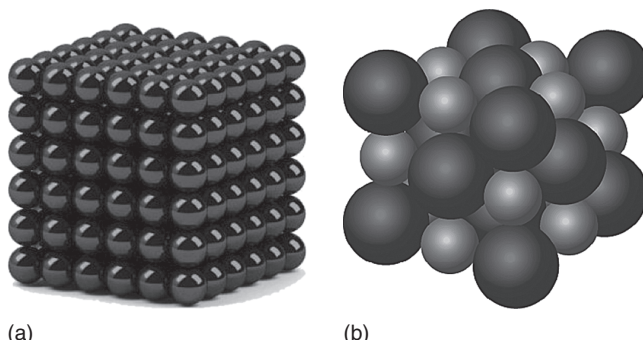


Figure 1.5 (a and b) Models of packing of spherical atoms as may appear in classical textbooks on crystallography and/or materials science.

has been studied over the whole range of packing fractions from near 0 to the maximum of 0.74 in three-dimensional space and also in higher dimensions. For packing fractions close to zero (simulating rarefied gases or stars in the Universe), the spheres can be considered as points distributed in space according to some law, for example the Poisson's linear point process. For small packing fractions (gases at normal or increased pressure), binomial distribution seems more appropriate. For packing fractions between approximately 0.40 and 0.74, the assemblies of spheres are models of liquids, amorphous (glasses), polycrystalline, and single-crystal solids. In this book, we shall be concerned with dense packings only (0.60–0.74). Examples of such packings from simulations are shown in Figure 1.6a and b.

This chapter contains the elementary geometrical and mathematical aspects required to define spheres, clusters of spheres and touching and non-touching neighbours, leading to assemblage of spheres usually referred to as *packing of spheres*. Methods for packing are described with a special emphasis on random arrangement of spheres. For this purpose, we approach the method of packing without any reference to a *lattice* (which is an essential crystalline concept). However, when appropriate, examples from regular and crystallographic arrangements are included for comparison and emphasis by contrast. To further remove any suggestion or inclination to lattice-like concepts, the packed aggregate of spheres will be presented as spherical in shape, and called *round cell*, rather than a cubic simulation cell used ubiquitously in computer simulations. The use of round cell should dissuade from any involuntary thought to perceive a lattice or to think of the edges of the cubic cell as indications of a lattice. To understand amorphous solids, one must disengage oneself from any crystallographic predilection.

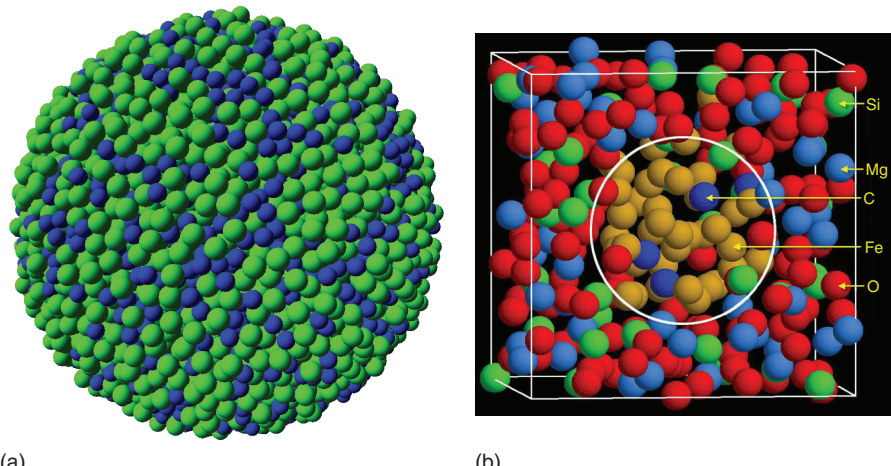


Figure 1.6 (a and b) Example of a round cell with random packing of spheres of two sizes, in comparison to a cubic cell with seemingly random packing of spheres of five sizes, from computer simulations.

1.2

Geometry of Spheres

1.2.1

A Sphere and Its Neighbours

In a general way, we call S_n a centrally symmetric convex body. Then a sphere of diameter, $D = 2R$, is defined in Euclidean space, E^n , by

$$S_n = \left\{ \mathbf{x} = (x_1, x_2, \dots, x_n) : \sum_{i=1}^n (x_i)^2 \leq \left(\frac{D}{2}\right)^2 \right\} \quad (1.2)$$

A sphere is a geometrical solid such that every point on its surface is at an equal distance from its centre. In three dimensions, points for which $(x_i)^2 = (x^2 + y^2 + z^2)_i < (D/2)^2$ is true, constitute the interior of the sphere, and all points for which $(x_i)^2 = (D/2)^2$ is true form the surface of the sphere.

In Cartesian space (E^3), if X is a set of points representing the centres of spheres, then we call,

$$S_3 + X \quad (1.3)$$

a packing of spheres in three dimensions.

Information about the character of the packing is contained entirely in the set X . The content of the set, which forms a list or a matrix, can be combined with additional information, such as *id* numbers of the spheres and the sphere's radii. Equation 1.3 is presented at this point to introduce the concept of neighbouring spheres. It will be considered in greater detail in the context of sphere packings later in this chapter.

Packing of spheres implies neighbours. We look for neighbours of spheres within primary clusters formed by the spheres. Let m be a positive integer, then an h -neighbour of a sphere (S_3) exists if,

$$X_i = \{x \in X : |x, x_i| \leq h\} \quad (1.4)$$

$$\text{where } X_i = \{x_{ij} : j = 1, \dots, m_i\} \quad (1.5)$$

In Equation 1.4, $|x, x_i| = |(x_i^2 - x_j^2)^{1/2}|$ denotes two-norm Euclidean distance between two points (centres of two spheres).

For hard, impenetrable (non-overlapping) spheres, $(x_i^2 - x_j^2)^{1/2} < D$, is disallowed for any i, j .

The case, $(x_i^2 - x_j^2)^{1/2} = D$, indicates touching neighbours i, j .

The number of neighbours and the distances between them define the geometrical character of the cluster and hence the packing.

The number of nearest neighbours is involved in considerations in condensed matter physics where the interactions between neighbours govern the physical properties. In dense packings, knowing about the number of nearest neighbours is important, and therefore, neighbouring spheres are categorized according to their

distance from the chosen central sphere. In particular, there are three categories that are used in physics of solids, and these are defined and described in detail:

- touching neighbours (by contact)
- neighbours by Voronoi tessellation (within a limited distance)
- neighbours by coordination shells (first, second, etc.) from radial distribution function

1.2.2

Neighbours by Touching

The first category is decided simply by the condition, $h = D$. Then, the h -neighbour is a touching neighbour. In this relationship, it is assumed that one sphere is at the origin ($x = 0$) and the other sphere is the neighbour.

The sphere at the origin will be referred to as the *inner sphere* and the touching sphere(s) will be called the *outer sphere(s)*. Within a packing, each outer sphere is in turn an inner sphere of its own cluster.

Two touching spheres meet at one point, the *contact point*, which belongs to the surfaces of both spheres, and lies on a straight line joining the centres of the two spheres. Conical projection of the outer sphere onto the surface of the inner sphere delineates a 'shadow' cup extended over the conical angle, $\pi/3$, associated with that contact point, as can be seen in Figure 1.7(a).

For two (or more) outer spheres touching the inner sphere, the contact points must have a minimum angular separation, that is their shadow cups must not overlap. We note that the contact points can be identified by radial vectors, \vec{R}_j , $j = 1 \dots k$, drawn from the centre of the inner sphere to the points on its surface, as shown in Figure 1.7(b).

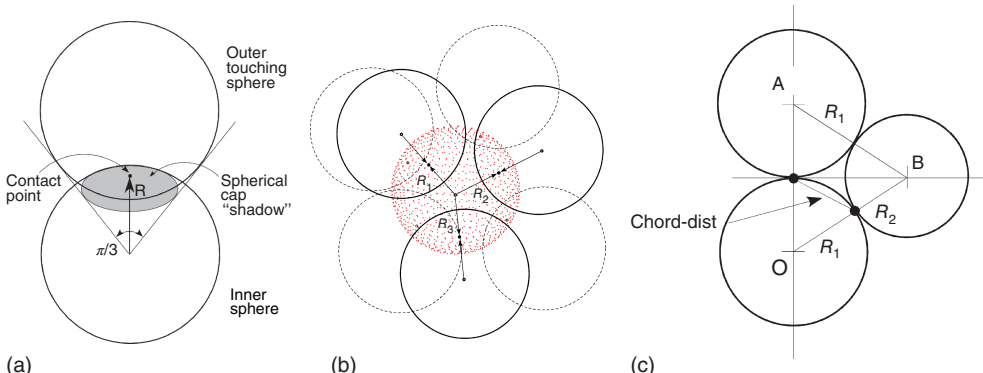


Figure 1.7 (a) Two spheres touching at a point, showing shadow of the outer sphere as a spherical cap on the inner sphere. (b) The exclusion angle shown for three outer

spheres. (c) Geometrical relationship for the chord distance between the contact points of unequal spheres. $OA = 2R_1$, whereas $OB = AB = R_1 + R_2$.

- Then the *angular separation*, expressed as

$$\text{angle, } \phi(R_i, R_j) = \arccos \left(\langle R_i, R_j \rangle / \frac{1}{4} D^2 \right) \quad (1.6)$$

between any two vectors emanating from the centre of the sphere, cannot be less than $\frac{1}{3}\pi$.

- In general, the condition

$$\frac{1}{3}\pi \leq \phi(\vec{R}_i, \vec{R}_j) \leq \pi, (1 \leq i < j \leq k); \quad (1.7)$$

must hold for any set of k outer spheres.

Another way to express the same condition is by means of the chord distance between the contact points on the surface of the inner sphere. In relation to Figure 1.7c, if the inner sphere (at O) has one of the touching spheres (at A) of radius, R_1 , and the other sphere (at B) of radius, R_2 , then the condition is expressed as follows:

$$\text{chord distance} \geq 2R_1 \sin \left(\frac{1}{2} \arcsin \sqrt{1 - \left(\frac{R_1}{R_1 + R_2} \right)^2} \right) \quad (1.8)$$

If $R_2 = R_1$, then from Equation 1.8 we calculate, $\frac{1}{2} \arcsin \sqrt{3/4} = 30^\circ$, so the minimum allowed chord distance = R_1 , which corresponds to a minimum angle of separation of 60° , in agreement with condition 1.7.

If $R_2 < R_1$, then the minimum distance will be correspondingly less. Finally, if $R_2 = 0$, then from Equation 1.8 we calculate, $\arcsin \sqrt{0} = 0^\circ$, so the minimum allowed chord distance is zero, as it should be.

Naturally, a sphere can have more than one touching neighbour. The number of touching neighbours, denoted by k , can vary in the range: $k_{\min} \leq k \leq k_{\max}$. In general,

- $k_{\min} = 1$, but $k_{\min} = 4$ when the packing is to represent a solid; see section on ‘fixed and loose spheres’,
- $k_{\max} = 12$ for spheres of the same size according to the so-called Kepler conjecture, and by common experience, but with formal proof achieved only recently (Hales, 1998).

Spheres of unequal sizes

Calculations have been carried out for k_{\max} in clusters in which the spheres are of unequal size. As the size of the inner sphere changes relative to that of the outer spheres, then the maximum possible number of outer spheres changes as is given in Table 1.1.

For clusters comprising multi-sized spheres, it is possible to estimate the maximum number of touching neighbours from Table 1.1 by interpolation.

Table 1.1 Maximum possible number of outer spheres of radius, R_2 , that can be in contact with inner sphere of radius R_1 over a selected range (Clare and Kepert, 1986).

Ratio, R_2/R_1	1.56	1.35	1.20	1.10	1.00	0.92	0.87	0.82	0.79
k_{\max}	8	9	10	11	12	13	14	15	16

1.2.3

Hard and Soft Spheres

Hard spheres are characterized by perfect rigidity, and consequently, a precisely defined radius, R . There is no attraction between hard spheres, but when brought in contact, the repulsive force diverges to infinity. In physical terms, this is described by a potential which varies with distance as shown in the following equation:

$$V_{hs} = \begin{cases} \infty & \text{for } r < R, \\ 0 & \text{for } r \geq R \end{cases} \quad (1.9)$$

The force between the spheres is derived from the potential: $f_{hs} = -\partial V_{hs}/\partial r$,

$$f_{hs} = \begin{cases} -\infty & \text{for } r < R, \\ 0 & \text{for } r \geq R \end{cases} \quad (1.10)$$

The variations of the potential and the corresponding force as a function of distance are shown in Figure 1.8.

Soft spheres are characterized by both repulsive and attractive potentials, of which the Lennard–Jones potential is a good example:

$$V_{ss} = V_{LJ} = 4\epsilon_0 \left[\left(\frac{\sigma}{r} \right)^m - \left(\frac{\sigma}{r} \right)^n \right] \quad (1.11)$$

In Equation 1.11, ϵ_0 is the depth of the potential energy well and σ is a parameter such that $V_{LJ} = 0$ when $r = \sigma$. The minimum, $V_{LJ} = -\epsilon_0$, occurs when $r = r_0 = (m/n)^{1/(m-n)}$ σ . The derivative of V_{LJ} with respect to r gives the interatomic force as

$$f_{LJ} = \frac{4\epsilon_0}{\sigma} \left[-m \left(\frac{r}{\sigma} \right)^{-m-1} + n \left(\frac{r}{\sigma} \right)^{-n-1} \right] \quad (1.12)$$

Both r_0 and ϵ_0 are specific to the given pair of interacting atoms. The exponents, m and n , define the strength of the repulsive and attractive forces, respectively. The most commonly used values that represent physical interactions are $m = 12$ and $n = 6$. Then, $r_0 = 2^{1/6} \sigma = 1.1225 \sigma$.

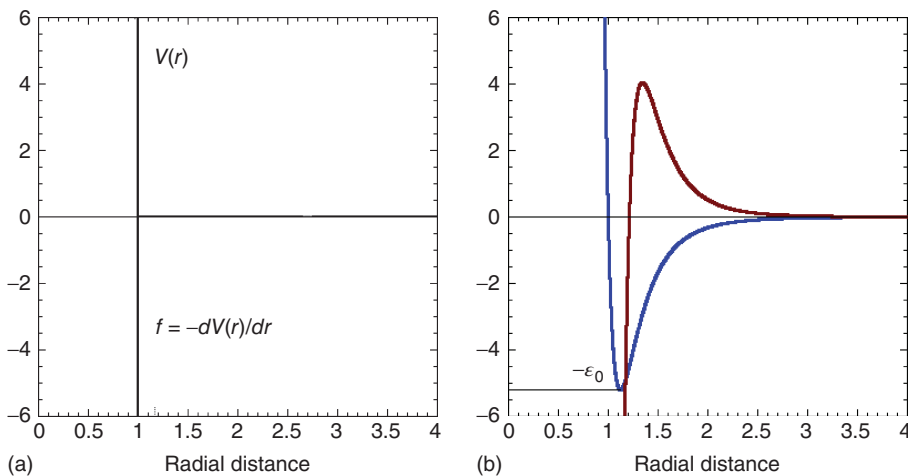


Figure 1.8 (a) Variation with distance of the potential and interatomic force for hard spheres. (b) Variation of L-J potential energy (with a minimum) and interatomic force (with a maximum) between two atoms.

The equilibrium separation of the two atoms defines the atomic radius. This assumption is reasonably accurate for metallic and van der Waals solids but may not be so for substances with covalent or ionic bonds in which the electronic structure of the atoms overlaps.

As a rule, hard spheres are used for modelling atomic arrangements by geometric packing, whereas soft spheres are used in molecular dynamics (MD) simulation of atomic arrangements and their properties.

Forces between particles

Force is the action of one body on another body. This may be direct as in body (surface) contact or through a force field (gravitation, magnetic, electrostatic, atomic, etc.).

Work, W , done by an applied force, \mathbf{F} , is evaluated at the start and end of the trajectory of the point of application. This means that there is a function $V(\mathbf{x})$, called a *potential*, that can be evaluated at the two points $\mathbf{x}(t_1)$ and $\mathbf{x}(t_2)$ to obtain the work over any trajectory between these two points. By convention, we define this function with a negative sign so that positive work is a reduction in the potential, that is,

$$W = \int_C \mathbf{F} \cdot d\mathbf{x} = \int_{\mathbf{x}(t_1)}^{\mathbf{x}(t_2)} \mathbf{F} \cdot d\mathbf{x} = V(\mathbf{x}(t_1)) - V(\mathbf{x}(t_2)) \quad (1.13)$$

The function $V(x)$ is called the *potential energy* associated with the applied force.

The application of the Nabla operator to the work function gives

$$\nabla W = -\nabla V = -\left(\frac{\partial V}{\partial x}, \frac{\partial V}{\partial y}, \frac{\partial V}{\partial z}\right) = \mathbf{F} \quad (1.14)$$

Because the potential V defines a force \mathbf{F} at every point x in space, the set of forces is called a *force field*. A particle in a forcefield may experience a force acting on it, depending on the character of the field and the properties of the particle.

Types of forces

- Long range – gravitational forces: a particle possessing mass, m will experience a force when in a gravitational field.

$$F = \frac{G(m_1 m_2)}{r_{12}^2}$$

- Electrical and magnetic forces: a particle possessing charge, q will experience a force when in an electrical field.

$$F = \frac{Q(q_1 q_2)}{r_{12}^2}$$

- Short range – interatomic forces as described in the following.

Interatomic forces

All intermolecular forces are directional as a rule, except those between two noble gas atoms. The induction and dispersion interactions are always attractive, irrespective of orientation, but the electrostatic interaction changes sign upon rotation of the molecules, that is depending on the mutual orientation of the molecules.

Thermal motion averages out electrostatic forces to a large extent because of rotation of the molecules. The thermal averaging effect is much less pronounced for the attractive induction and dispersion forces.

London dispersion forces, named after the German–American physicist Fritz London, are forces that arise between instantaneous multipoles in molecules without permanent multipole moments. These forces dominate the interaction of non-polar molecules and also play a less significant role in van der Waals forces.

The van der Waals force between two spheres of constant radii is a function of separation as the force on an object is the negative of the derivative of the potential energy function, $F_{\text{VW}}(r) = -(dV(r))/dr$.

The Lennard–Jones potential, expressed in Equation 1.11, is a mathematically simple model that approximates the interaction between a pair of neutral atoms or molecules. The repulsive r^{-12} term describes Pauli repulsion at short ranges because of overlapping electron orbitals. It is used because it approximates the Pauli repulsion well and is convenient for computational efficiency of calculating r^{12} as the square of r^6 . The attractive r^{-6} term describes attraction at long ranges.

The Buckingham potential, expressed in Equation 1.15, is a formula that describes the Pauli repulsion energy and van der Waals energy, for the interaction of two atoms.

$$\Phi_{12}(r) = A \exp(-Br) - \frac{C}{r^6} \quad (1.15)$$

A , B and C are constants of the particular atomic pair. The two terms on the right-hand side constitute a repulsion and an attraction because their

first derivatives with respect to r are negative and positive, respectively. R. A. Buckingham proposed this as a simplification of the Lennard–Jones potential in a theoretical study of gaseous helium, neon and argon.

With the L–J potential, the number of atoms bonded to an atom does not affect the bond strength. The bond energy per atom therefore increases linearly with the number of bonds per atom. Experiments show instead that the bond energy per atom increases quadratically with the number of bonds.

$$V(r) = 4\epsilon[12\sigma^{12}/r^{13} - 6\sigma^6/r^7] \quad (1.16)$$

Many-atom potentials developed in the 1980s allow to model dense solids where bonds become weaker as a consequence of Pauli principle, due to local environment becoming crowded. Density functional theory (DFT) is a quantum mechanical modelling method used to model the structure of atoms, molecules and condensed phases.

1.3

Geometry of Clusters

The inner sphere (1) and its (k) touching neighbours form a *primary* or local ($1 + k$) cluster. Thus, a cluster composed of identical spheres is specified uniquely by four parameters.

- 1) the radius of the sphere (or spheres)
- 2) the number of the touching spheres, k , also called the *coordination number*
- 3) the disposition (or positioning) of the outer spheres, defined by the contact points
- 4) the orientation of the cluster in space

1.3.1

Regular Clusters

In Mathematics, a regular shape refers to a polygon that has all its sides equal and all its angles also equal. Perfect examples are squares and an equilateral triangle, where all the angles and sides are equal. A regular solid object has equal sides and equal angles, so that all its faces are regular polygons.

The smallest regular primary cluster is composed of $(1 + 4)$ spheres and has tetrahedral geometry, as shown in Figure 1.9.

The geometry of this cluster is specified by

- 1) the radius of each sphere = 1
- 2) the coordination number of the inner sphere, $k = 4$
- 3) the angular separation between each pair of adjacent outer spheres, $\phi = 2 \arcsin \sqrt{2/3} = 109.47^\circ$
- 4) the orientation of the cluster can be specified with respect to any of its four axes of twofold and four axes of threefold symmetry.

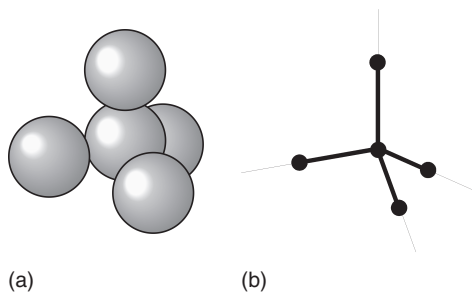


Figure 1.9 (a and b) Regular cluster of tetrahedral geometry ($k = 4$) and its minimum outline representation.

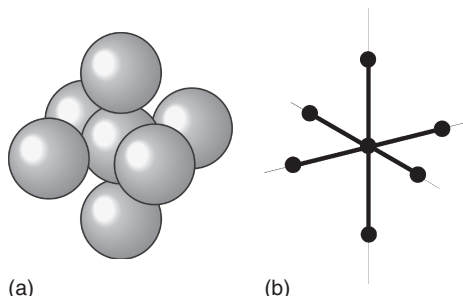


Figure 1.10 Regular cluster of cubic geometry ($k = 6$) and its minimum outline representation.

Rotation of the cluster around any of the rotational axes makes the new cluster indistinguishable from its original image, which is the property of rotational symmetry.

Another example of a regular cluster is of cubic geometry, as shown in Figure 1.10

The geometry of this cluster is specified by:

- 1) the radius of each sphere = 1
- 2) the coordination number of the inner sphere, $k = 8$
- 3) the angular separation between adjacent spheres, $\phi = \pi/2 = 90^\circ$
- 4) the orientation of the cluster can be specified with respect to either its four \times threefold, three \times fourfold or six \times twofold axes of symmetry.

We can generalize the property of rotational symmetry by stating that the rotation of any regular cluster by the angular separation makes the rotated cluster indistinguishable from its original image.

Clusters derived from crystalline structures have a well-defined number of outer spheres. The very special and unique arrangements of spheres in these clusters arise because the number of neighbours and separation angles assume precise values, as given in Table 1.2.

Table 1.2 Separation angles between nearest outer spheres in selected regular clusters.

Cluster name	Neighbours, k	Separation angle, ϕ
hcp, fcc and icosahedral	12	$\pi/3 = 60^\circ$
Body-centred cubic (bcc)	8	$\pi/3 = 60^\circ$
Simple cubic (sc)	6	$\pi/2 = 90^\circ$
Tetrahedral (th)	4	$2 \arcsin \sqrt{2/3} = 109.47^\circ$

It can be accepted, either from prior knowledge or even only intuitively at this stage, that regular clusters cannot be arrived at by random addition of spheres to the inner sphere; there must be some special forces at play to influence the existence of these special, unique arrangements. In the field of crystallization, these forces derive from minimization of Gibbs free energy; in physical flow of balls, it is the gravitational force that contributes to formation of ordered clusters, and so on.

That such forces are required can be understood with the help of the following example. The probability of throwing the number, say 3, with a standard dice is $1/6$. One can make a dice with 12 faces, then the probability of throwing 3 is $1/12$; for a dice of 24 faces, the probability is $1/24$. In the special case when the dice has an infinite number of faces (i.e. a perfect sphere), the probability becomes $1/\infty = 0$. Therefore, a perfect cluster of fcc structure, or any other ordered cluster of spheres which requires achieving singular values of the separation angles, cannot be created by a random processes.

In mathematical statistics, if X is a continuous random variable, then it has a probability density function $f(x)$, and therefore, its probability of falling into a given interval, say $[a, b]$ is given by the integral,

$$\Pr[a \leq X \leq b] = \int_a^b f(x) dx \quad (1.17)$$

In particular, the probability for X to take any single value a , such that $a \leq X \leq a$, is zero, because an integral with coinciding upper and lower limits is always equal to zero.

1.3.2

Irregular Clusters

If external force fields do not exist, formation of a cluster around a central sphere by addition of spheres at random can only result in a random configuration of the cluster. The number of ways that packing arrangements can occur depends on the space that is free to be occupied and the number of spheres available for packing.

An example of an irregular cluster is shown in Figure 1.11. The radius of each sphere can be specified (say, 1), and the coordination number of the inner sphere can be determined (say, $k = 7$). However, an irregular cluster has no axis of symmetry; therefore, the separation angles of the outer spheres will be different for

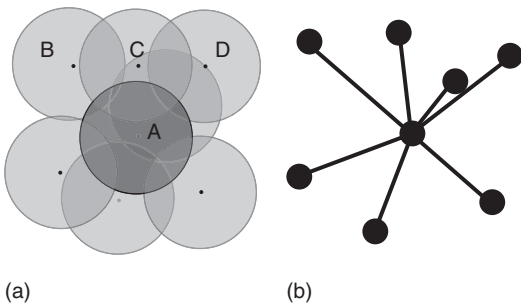


Figure 1.11 (a and b) A cluster with irregular geometry.

each pair of outer spheres, and the orientation of the cluster in space can only be specified by giving the positions (contact points) of all outer spheres.

Furthermore, as a random assemblage of spheres is composed of random (irregular) clusters where each primary cluster is different from every other primary cluster, it follows that in random packing the clusters must have:

- a distribution of the number of touching neighbours; and
- a distribution of their positions (or equivalently, a distribution of separation angles).

Next we present statistical models for the formation of random clusters.

1.3.3

Coordination of $(1 + k)$ Clusters

The term *coordination number* was defined originally in 1893 by Alfred Werner (Swiss chemist) as the total number of neighbours of a central atom in a molecule. The emphasis is on bonding structure in molecules or ions and the coordination number of an atom is determined by simply counting the other atoms to which it is bonded (by either single or multiple bonds). For example, $[\text{Cr}(\text{NH}_3)_2\text{Cl}_2\text{Br}_2]^-$ has Cr^{3+} as its central cation, which has a coordination number of 6.

Coordination number was adopted in crystallography and materials science to be the number of atoms touching a given atom in the interior of a crystal. For example, iron at room temperature has a body-centred cubic (bcc) crystal structure. Each iron atom in the interior occupies the centre of a cube formed by eight neighbouring iron atoms. The bulk coordination number for this structure is therefore 8. However, for an atom at a surface of a crystal, it is defined as the surface coordination number. For example, an atom lying on a [110] plane of iron exposed to the surface will have only six touching atoms, and correspondingly, its coordination number will be 6.

In random packing of spheres, two mathematical models are presented for predicting the coordination number, or rather for the distribution of coordination numbers in a large sample of random clusters:

- the so-called blocking model formed by sequential addition of spheres to the central inner sphere until no more spheres can be added
- the so-called distributed loose sphere model based on the fact that, as a rule, random clusters have lower density of packing than the possible maximum for close packed ordered clusters.

1.3.3.1 Blocking Model for Cluster Formation

Consider the construction of a $(1 + k)$ random cluster by sequential addition of spheres to the surface of the inner sphere. The problem can be approached with the following question: What is the probability, $P(k)$, that k spheres can be added in this way onto random positions of the inner sphere, subject to the exclusion condition.

For two spheres touching the inner sphere, the contact points must have a minimum angular separation, as specified by Equation 1.7. Bearing in mind this limitation, we consider the addition of a sphere as equivalent to occupying a spherical cap on the inner sphere, centred on the contact point and resting on a cone with a vertex angle of $\phi = \pi/3$. The solid angle of a cone with apex angle $\phi/2$ is equal to the area of a spherical cap on a unit sphere,

$$\Omega = 2\pi(1 - \cos \phi/2) \quad (1.18)$$

Then, the probability that another sphere can be added is equal to 1 for as long as there is a spherical cap with a minimum area Ω left free on the surface of the inner sphere. This is always true for $1 \leq k \leq 5$, regardless of the placement of the k spheres.

For $k \geq 6$, the probability will vary, depending on the disposition of the previously added spheres. As each spherical cap has an associated concentric exclusion zone extended to an angle $2\pi/3$, the minimum probability, $P_{\min}(k)$, will occur when the zones are distributed (positioned) as far from each other as possible (i.e. equi-spaced), and the maximum probability, $P_{\max}(k)$, will occur when their respective exclusion zones overlap to their maximum extent. Therefore, the actual probability will depend on k and be limited to

$$P_{\min}(k) \leq P(k) \leq P_{\max}(k) \quad (1.19)$$

Naturally, for $k = 1$, $P(k) = 1$ and for $k = 12$, $P(k) = 0$. One must find the values of $P(k)$ for all other values of k .

Apparently, there is no general analytical solution to this problem. Instead, it is relatively simple to set up a computer program to carry out such sequential addition of spheres and to sum the frequencies of the successful events. Such computations have been carried out and the results, based on 10^5 cluster samples, are shown in Figure 1.12(a). By this method, we find that the probability of random clusters with coordination of eight to nine is over 85% and the average coordination number is $\bar{k}_B = 8.29$.

The computational process involves two stages. In stage one, the surface of the inner sphere is divided into n equally spaced points, as shown in Figure 1.13. This is a well-established procedure in mathematical geometry (Conway and Sloane,

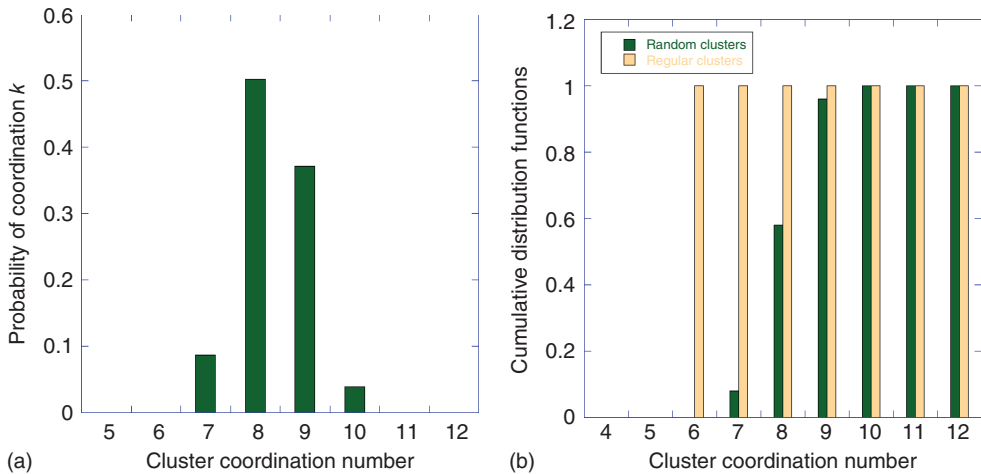


Figure 1.12 Statistics for 10^5 random clusters. (a) Probability of coordination in random clusters. (b) The corresponding blocking function.

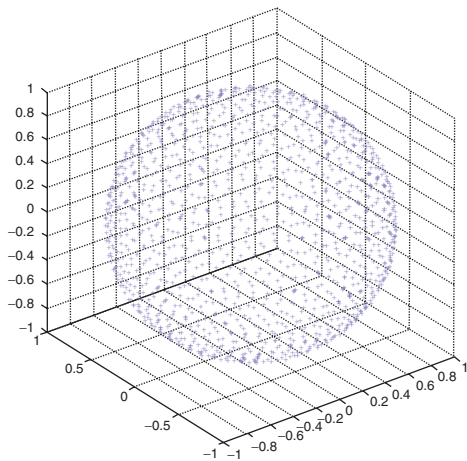


Figure 1.13 A sphere whose surface has 1000 equi-spaced points on its surface.

1998), and a ready made code has been published by Leopardi (2006). Then, from the created list of n points, a particular point is selected at random, and condition 1.7 is tested. If it is satisfied, then an outer sphere is added to (made to touch) the inner sphere at that point. If the condition is not satisfied, then the point is rejected and the program continues to loop with further spheres added until no more can be added. The data of such randomly created clusters are collected, and the summary statistics are shown in Figure 1.12(a).

We call this discrete function the *coordination number distribution function* derived from the blocking model, denoted $\Psi_B(k)$.

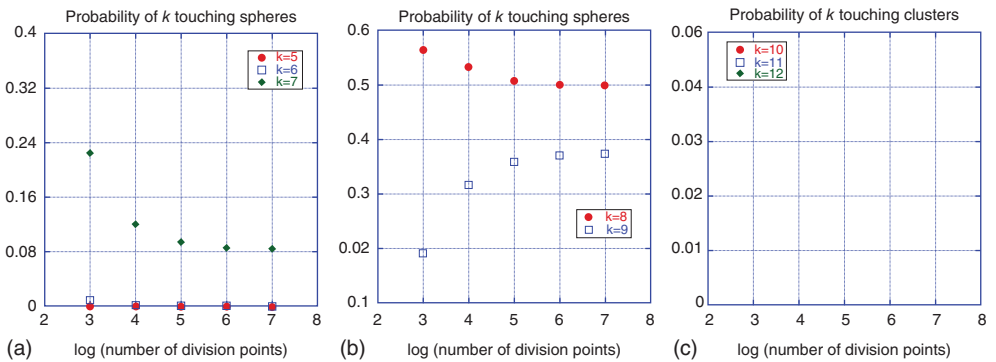


Figure 1.14 (a–c) Coordination dependence on a number of division points.

The coordination probability of clusters created by this method depends on the number n of the sphere division points. This dependence is shown in Figure 1.14. If the number is small (for example 8), then all created clusters will be regular with coordination 8. If the number is $n = 20$, then the created clusters will be random but the points for addition of spheres are quickly exhausted and the distribution will be limited. With increasing n , the randomness of positioning of the spheres increases. In principle, a perfectly random distribution would be obtained for $n = \infty$. The plot in Figure 1.12(a) gives the asymptotic values of probability for $n \geq 10^7$.

We can redefine the cluster creation problem with reference to the so-called *blocking number* (Barlow, 1883, Zong, 1999). For a regular cluster of equal size spheres, the blocking number is 6. It is known that a regular simple cubic pattern is sufficient to block the inner sphere from the addition of any more outer spheres. However, a random arrangement of six outer spheres is unlikely to completely block the inner sphere, and the blocking will vary from cluster to cluster. By definition, complete blocking occurs when there is not a single spherical cap area left on the surface of the inner sphere.

The concept can be generalized to both random and regular clusters by defining a *blocking function*,

$$\hat{b}(k) = \sum_k P(k) \quad (1.20)$$

For regular clusters, the blocking function, \hat{b} , has a sharp transition: $\hat{b} = 0$ for $k \leq 5$ and $\hat{b} = 1$ for $k \geq 6$, as indicated in Figure 1.12b by the gold bars.

For irregular clusters, the corresponding blocking function, also included in the graph, is shown by the dark green bars. This blocking function assumes the values $\hat{b}(k \leq 5) = 0$ and then increases gradually in the interval $6 \leq k \leq 9$, for $k = 11$ $\hat{b}(k) \cong 1$, finally achieving the value $\hat{b}(k = 12) = 1$.

Suppose we consider the blocking function (Equation 1.20) to be the CDF of the probability of occurrence of clusters with k outer spheres,

$$\text{CDF}(k) = \hat{b}(k) = \sum_k P(k) \quad (1.21)$$

Table 1.3 Probability of coordination and the corresponding blocking function for clusters created by random sequential addition of spheres.

k	$P(X \leq k)$	$CDF = \Psi_b(k)$
1	0	0
2	0	0
3	0	0
4	0	0
5	0	0
6	0.009	0.009
7	0.08	0.089
8	0.50	0.589
9	0.37	0.959
10	0.038	0.997
11	0.003	0.9999
12	0	1.0

Then, the following Table 1.3 can be constructed from the results displayed in Figure 1.12.

The cumulative distribution function, CDF, of a real-valued random variable X is the function given by

$$CDF_X(x) = P(X \leq x) \quad (1.22)$$

where the right-hand side represents the probability that the random variable X takes on a value less than or equal to x . The probability that X lies in the semi-closed interval $(a, b]$, where $a < b$, is therefore:

$$P(a < X \leq b) = CDF_X(b) - CDF_X(a) \quad (1.23)$$

If X is a purely discrete random variable, then it attains values x_1, x_2, \dots with probability $p_i = P(x_i)$, and the CDF of X will be discontinuous at the points x_i and constant in between:

$$CDF(x) = \sum_{x_i \leq x} P(X = x_i) = \sum_{x_i \leq x} p(x_i) \quad (1.24)$$

1.3.3.2 Fürth Model for Cluster Formation

Another possible distribution comes from an argument initially proposed by R. Furth (1964) in connection with studies of the structure of liquids by J. D. Bernal. We describe this process via the following three variables:

- 1) k , the number of neighbour-touching spheres relative to each inner sphere;
- 2) x , the maximum number of *sites* for spheres in dense packing that can be in contact with the inner sphere; and
- 3) s , the number of *virtual sites* available to spheres in a less dense packing.

In general, $s \geq x \geq k$. From elementary combinatorics, k spheres can be placed in x sites in $\binom{x}{k}$ ways, and $x - k$ (empty) sites can be chosen from $s - x$ in $\binom{s-x}{x-k}$

ways, whereas x sites can be distributed over s sites in $\binom{s}{x}$ ways. The probability of k spheres touching the inner sphere amongst the s sites subject to the maximum nearest-neighbour constraint, is thus

$$\begin{aligned} P(k) &= \Psi_F(k, s) = \binom{x}{k} \binom{s-x}{x-k} \binom{s}{x} \\ &= \frac{x!(s-x)!^2}{k!s![(x-k)!]^2(s+k-2x)!} \end{aligned} \quad (1.25)$$

Now, assume that the number of possible sites is related to the available space around the inner sphere. Specifically, suppose that

$$s = x(v_h''/v_h') \quad (1.26)$$

where $v_h = V_V - v_s = v_s(1 - p_f)/p_f$, V_V if the volume of the Voronoi cell, v_s is the volume of an inscribed sphere, and p_f is the packing fraction. In relation 1.26, the prime corresponds to close packing with $s = x = k = 12$ and a corresponding maximum packing density, and the double prime corresponds to a less dense random packing for which $s > x > k$, for which the function $\Psi_F(k)$ will have a non-degenerate distribution. Combining these relations with Equation 1.26 gives a formula for s :

$$s = x \left(\frac{p_f'(1 - p_f'')}{p_f''(1 - p_f')} \right) \quad (1.27)$$

For close packing, $x = 12$ and $p_f' = \pi/\sqrt{18} \approx 0.74$. For lower density random packing, we assume $p_f'' = 0.62$. Substitution of these values in formula 1.27 gives $s \approx 20.9$. Taking the closest maximum whole number, $s = 21$, formula 1.25 can be now evaluated. The result is a multi-valued discrete function showing a prevalence of coordination numbers 6, 7 and 8 as shown in Figure 1.15. Other cases for $s = 17$ to 20 have been evaluated and are given in Table 1.4.

We call this discrete function the Fürth coordination number distribution function derived from the loose sphere model, denoted $\Psi_F(k)$.

Consequent on random packing is variation of coordinations in clusters, with admissible values in the range, $4 \leq k \leq 12$. If $c(k)$ is the fraction of clusters with a given contact number, k , then for the whole packed body of spheres, $\sum c(k) = 1$, summed for $k = 4, \dots, 12$. Then, the average number of contacts per sphere is $\bar{k} = \sum k c(k)$, typically a non-integer, and possibly an irrational number. The average coordination number for this distribution is $\bar{k}_F = 6.91$.

In contrast to the blocking model, this model allows coordination numbers of 4 and 5, with 7 being the most frequent. In support of this observation, we can say that clusters with such low values of touching spheres are possible if they are stabilized by the next nearest-neighbour spheres, that is spheres existing within the s virtual sites around the inner sphere. It will be shown later that these are so-called Voronoi nearest neighbours.

In view of the distribution of coordination numbers, one can assume that in a packing, clusters with k values higher than \bar{k} will be surrounded by clusters with

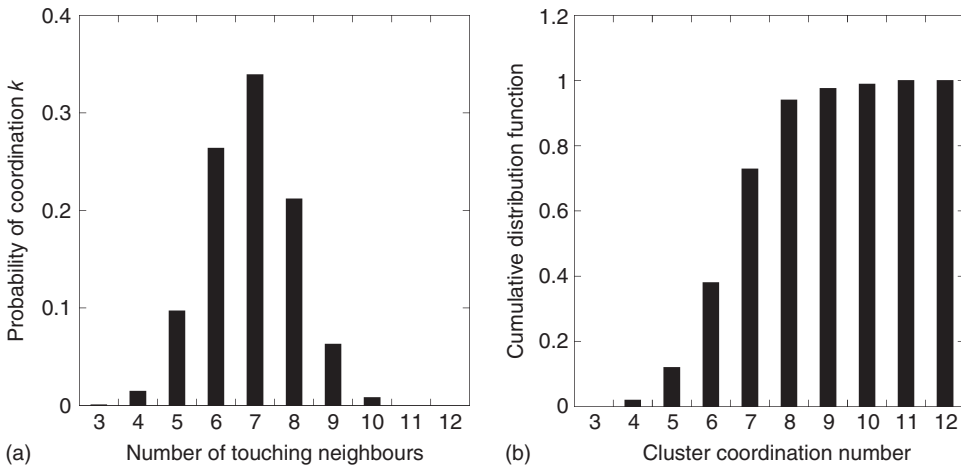


Figure 1.15 (a and b) Coordination distribution function, $\Psi_F(k)$, of random clusters predicted by Equation 1.25 and its cumulative distribution function (CDF).

Table 1.4 Computed values of the $\Psi_F(k)$ function for the selected values of the parameter s as shown.

k	$s = 21$	$s = 20$	$s = 19$	$s = 18$	$s = 17$
3	0.000748	0	0	0	0
4	0.015157	0.003930	0	0	0
5	0.097003	0.050298	0.015718	0	0
6	0.264060	0.205380	0.128360	0.049774	0
7	0.339510	0.352080	0.330080	0.255980	0.127990
8	0.212190	0.275070	0.343830	0.399970	0.399970
9	0.062872	0.097801	0.152810	0.237020	0.355530
10	0.008084	0.014670	0.027507	0.053329	0.106660
11	0.000367	0.000762	0.001667	0.003879	0.009696
12	0	0	0	0	0.000162
Sum =	1.000000	1.000000	1.000000	1.000000	1.000000

k values lower than \bar{k} , and vice versa, so that the full range of clusters is used, allowing for density fluctuations across the body of spheres.

In probability theory and statistics, the hypergeometric distribution (Equation 1.25) is a discrete probability distribution that describes the probability of successes in draws without replacement from a finite population of size containing a maximum of successes Figure 1.16.

The CDF of X will be discontinuous at the points k_i and constant in between:

$$\text{CDF}(k) = \sum_{k_i \leq k} P(X = k_i) = \sum_{k_i \leq k} \Psi_F(k) \quad (1.28)$$

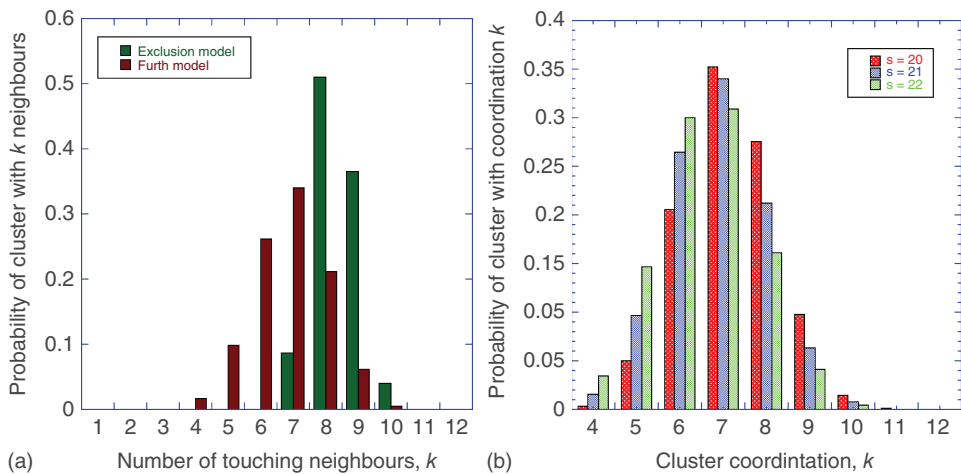


Figure 1.16 (a) Comparison of the distributions, Ψ_B and Ψ_F for randomly created clusters of equal-sized spheres. (b) Comparison of probabilities for clusters based on Equation 1.25 for s values as indicated.

For two-sized spheres, the result will depend on the relative size and whether smaller spheres touch a larger sphere or the other way round (Table 1.1).

1.3.4

Configuration of $(1 + k)$ Clusters

1.3.4.1 Regular Clusters

In the theory of crystallography, the symmetry elements of the unit cell describe the configuration of a given cluster. For example,

- hcp configuration with at least one axis of sixfold rotational symmetry (Figure 1.17a)
- fcc configuration with at least six axes of fourfold rotational symmetry and eight axes of threefold rotational symmetry (Figure 1.17b)
- bcc configuration with similar symmetry elements to that for fcc.

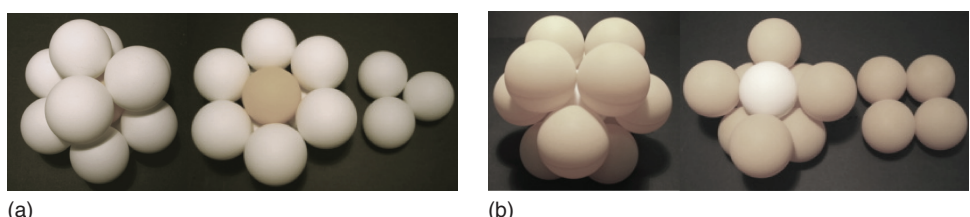


Figure 1.17 (a and b) Atomic arrangements in clusters of crystalline form: hcp (3+6+3) layers and fcc (4+4+4) layers, showing the complete cluster and its components.

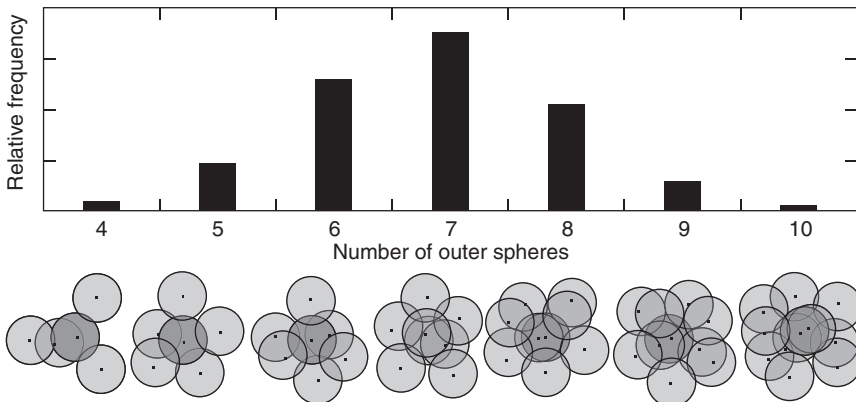


Figure 1.18 Examples of irregular clusters of equal-sized spheres with $k = 4$ to $k = 10$. Above, their relative frequency when randomly created by the Fürth method.

Therefore, the configuration of regular clusters is defined entirely by the symmetry elements of the corresponding crystal, although a primary cluster is a subset of the unit cell, and may have fewer symmetry elements than the unit cell itself.

Most importantly, the configurations of all crystalline clusters (unit cells) of a given form are exactly the same, although the size and chemistry may differ.

1.3.4.2 Irregular Clusters

In contrast to crystalline clusters, clusters created by a random process are different from each other even in the same (solid) substance. These variations are in terms of the number of touching neighbours, k , in the disposition of the outer spheres and their orientation in space. In theory, there will be an infinite variety of clusters and no two clusters alike. We refer to the positioning of the outer spheres as the *configuration* of the cluster. The orientation of the cluster in space is not important at this stage. Their appearance and relative number is shown in Figure 1.18.

For two clusters ($\ell = 1$ and $\ell = 2$) to be identical, we should necessarily have $k_1 = k_2$, $\zeta_1 = \zeta_2$ and $\Omega_1 = \Omega_2$ for the coordination number, the closing vector and spatial orientation, respectively.

Each cluster has nine possible values of k : 4, ..., 12. If the distribution of k is equiprobable, then the probability that two clusters have the same number of contact points (the same value of k) is $\sum_{k=4}^{k=12} (1/9)^2$.

For any given distribution $\Psi(k)$, we can write more generally that the probability for two clusters to have the same value of k is $\sum_{k=4}^{k=12} [\Psi_k]^2 = \frac{1}{9}c$, where $1 \leq c \leq 9$ is a constant. Next, we find that the probability of the two closing vectors to be the same as zero as ζ is a continuous variable. The same applies to Ω . Consequently, the probability of finding two identical clusters, if taken at random from a large (infinite) collection of random clusters, is zero.

Now, we turn our attention to the definition of the configuration of random clusters, which can be specified either individually for any given cluster or

collectively for all clusters by appropriate statistics. The configuration of a cluster can be defined in two ways:

- by radial vector construction
- by spherical harmonics

1.3.4.3 Closing Vector Based on Radial Vector Polygon

This new method was conceived specifically to describe the configuration of random clusters and is capable of defining the configuration of an individual cluster, as well as describing the statistics of a large collection of random clusters (To *et al.*, 2006). In that sense, it provides a quantitative measure of a cluster's configuration in the absence of any regularity and symmetry elements. As an example, we take a cluster comprising nine outer spheres as shown in Figure 1.19a. For the given cluster, we identify the contact points between the inner and outer spheres by radial vectors, $\vec{R}_j, j = 1, \dots, k$, drawn from the centre of the inner sphere to the contact points on its surface as shown in Figure 1.19b. The contact points bisect the distances from the centre of the inner sphere to the centres of its touching neighbours.

Note that the positions of the contact points on the surface of the inner sphere are sufficient to define the configuration of the whole cluster uniquely and adequately. From now on, we focus on the properties of the inner sphere alone, bearing in mind that the sphere with its contact points represents the whole cluster.

For the purpose of analysis, we may arbitrarily number the contact points and align the contact point numbered 1 with the vertical axis of the external reference system, as shown in Figure 1.19b.

Then, the quantitative measure of the configuration of the cluster is defined in terms of a vector polygon with vertices R_j :

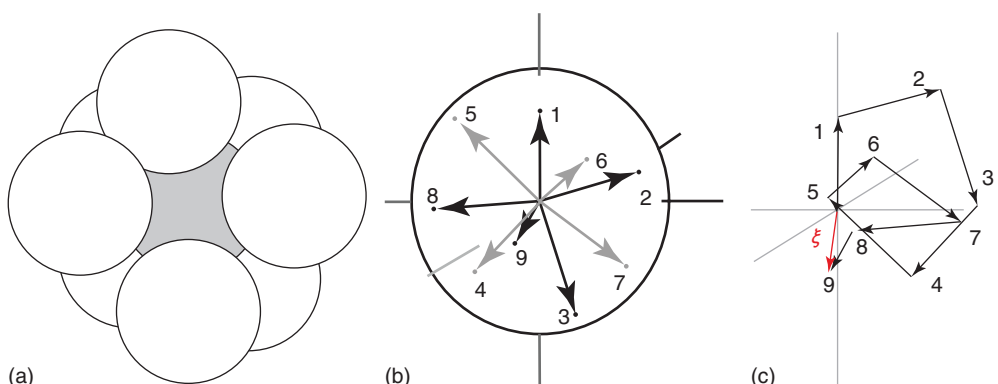


Figure 1.19 (a) An irregular (1 + 9) cluster. (b) The inner sphere of the irregular cluster, showing contact points and radial vectors. (c) A vector polygon constructed from the radial vectors.

$$\vec{\zeta} = \sum_{j=1}^{\kappa(x_\ell)} \vec{\mathbf{R}}_j \quad (1.29)$$

where x_ℓ represents the ℓ 'th sphere and κ is its corresponding number of its touching contacts. The sum represents a chain of the radial vectors and $\vec{\zeta}$ is the closing vector of the three-dimensional vector polygon.

The same vector construction can be applied to any and all clusters; therefore, the configurations of all clusters can be characterized by this method.

As the contact points are randomly positioned on the sphere, the vector polygon represents a *random walk* in three-dimensional space. A random walk is a sequence of random steps with independent and identically distributed increments. In mathematical analysis, there are two important questions relating to random walks:

- What is the end-to-end distance of a random walk consisting of n number of steps?
- What is the most probable end-to-end distance of such a random walk if the specific steps are not defined, but the number of the steps is known?

The answer to the first question is given by Equation 1.29. The answer to the second question is of statistical nature and is considered below.

Random walks

Random walk is an action involving consecutive jumps in space from point to point. The end of one step is the beginning of the next step, thus forming a continuous chain of steps or links. Each link can be represented as a vector of length, \vec{a} . The interest is to predict mathematically the so-called end-to-end distance after n steps.

Let the position of the walker be denoted by \mathbf{R}_n .

If the direction of each link is random and independent of the direction of the previous link, then the random walk is called *Gaussian random walk*.

The term random walk was first introduced into scientific literature by Karl Pearson in 1905 in relation to the spread of malaria by mosquitos. Random walks can explain the observed behaviour of processes in fields such as ecology, economics, psychology, computer science, physics, chemistry, and biology.

Consider a simple random walk of equal steps as shown in Figure 1.20. Let the length of the step be $a = |\vec{a}|$. After n number of steps, the end-to-end vector distance of the walk, denoted as \vec{L} , is given by

$$\vec{L} = \sum_{i=1}^n \vec{a}_i \quad (1.30)$$

The square of the magnitude of the end-to-end distance is equal to

$$|\vec{L}|^2 = \sum_{i=1}^n a_i \sum_{j=1}^n a_j = \sum_{i=1}^n a_i^2 + 2 \sum_{j=1}^n a_i a_j \quad j \neq i \quad (1.31)$$

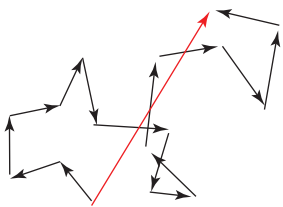


Figure 1.20 Random walk and its end-to-end distance.

This quantity is always positive regardless of direction. It may assume values in the range from 0 to $n a$. However, the statistical quantity, known as *the mean square end-to-end distance*, gives the most probable distance:

$$\langle L^2 \rangle^{1/2} = a\sqrt{n} \quad (1.32)$$

where the $\langle \rangle$ brackets indicate statistical average.

The second term in Equation 1.31 is equal to $a^2 \times \cos(\angle_{ij})$, where \angle_{ij} is the angle between two adjacent step vectors. If the orientation of the steps is completely random and uncorrelated (the so-called freely jointed chain), then the statistical average $\sum \cos(\angle_{ij}) = 0$, and therefore the second term is equal to zero, leaving only the first term.

Categories of random walks:

Gaussian random walk (GRW) – carried out in unlimited space, with the direction of each step independent of previous steps. $\langle L^2 \rangle \sim n$.

Self-avoiding random walk (SARW) – similar to GRW, but previously occupied points cannot be occupied again and each point has excluded space around it that cannot be occupied by other steps. Consequently, the mean square end-to-end distance becomes larger: $\langle L^2 \rangle \sim n^{6/5}$.

Self-avoiding space limited random walk (SASLRW) – similar to SARW, but the space for executing random walk is limited (finite), and therefore, the walk must terminate when the available space is used up. No general analytical solution exists. A possible relationship is $\langle L^2 \rangle \sim n^{6/5} \exp\left(-\frac{\gamma}{1-n/n_{\max}}\right)$, where γ and n_{\max} are constants specific to the random walk.

We also define a function, ζ , equal to the magnitude of the vector, $\vec{\zeta}$:

$$\zeta(k) = \zeta = \left\| \vec{\zeta} \right\| \quad (1.33)$$

Then, ζ is a summary statistic of any particular local cluster.

It should suffice to state that for any number and arrangement of contact points, that is for any number of random clusters, the ζ -function assumes values in a finite interval:

$$[0 \leq \zeta \leq \zeta_{\max}(\kappa(x_\ell))] \quad (1.34)$$

For each value of the number $k = 4, \dots, 12$, there is a unique maximum value of the ζ -function = $\zeta_{\max}(k)$. This value corresponds to an arrangement in which

Table 1.5 Calculated values of $\zeta_{\max}(k)$, and $\zeta_{\max}^{\text{fixed}}(k)$. For $k = 7$ & 11 by interpolation. Penultimate row for icosahedral. Last row for fcc and hcp.

k	$\zeta_{\max}/(R)$	$\zeta_{\max}^{\text{fixed}}/(R)$
1	1	Not applicable
2	$\sqrt{3}$	Not applicable
3	$\sqrt{2}\sqrt{3}$	Not applicable
4	$\frac{5}{3}\sqrt{3}$	$\sqrt{3}$
5	$\sqrt{3}\sqrt{3}$	$\sqrt{2}\sqrt{3}$
6	$\frac{4}{3}\sqrt{2}\sqrt{3}$	$\frac{5}{3}\sqrt{3}$
7	$\sqrt{3}\sqrt{3}$	$\sqrt{3}\sqrt{3}$
8	$2\sqrt{2}$	$2\sqrt{2}$
9	$\sqrt{3}\sqrt{2}$	$\sqrt{3}\sqrt{2}$
10	$\sqrt{3}$	$\sqrt{3}$
11	1	1
12 _{ico}	≈ 0	≈ 0
12 _{fcc,hcp}	0	0

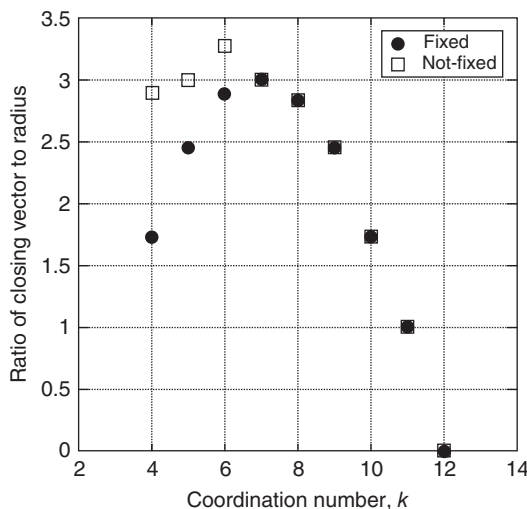


Figure 1.21 A plot of the closing vector values for fixed and non-fixed spheres from Table 1.5.

the outer spheres are rolled on the surface of the inner sphere towards the south pole into a close packed arrangement. The values of $\zeta_{\max}(k)$ have been calculated according to this approach and are listed in Table 1.5. A plot of the closing vectors for the two conditions, not-fixed and fixed, is shown in Figure 1.21.

If the further condition is imposed requiring that the inner sphere be fixed by the outer spheres, then the values of $\zeta_{\max}(k)$ change correspondingly to $\zeta_{\text{fix}}(k)$, as

given in Table 1.5, third column. These values were calculated assuming that one of the outer spheres moves to a position diametrically opposite another touching sphere, so that for $k = 4$ we have only two radii (separated by an angle $\frac{1}{3}\pi$) contributing to the value of $\zeta_{\text{fix}}(4)$, for $k = 5$ only three radii, and so on. (The actual values must be arbitrarily smaller as the sphere has to be on the other hemisphere, however imperceptibly). Consequently, for fixed spheres, condition 1.34 is finally expressed as

$$[0 \leq \zeta \leq \zeta_{\text{fix}}(\kappa(x_\ell))]. \quad (1.35)$$

A vector polygon formed by a chain of radial vectors according to Equation 1.29 can be considered in terms of a random walk in space. We note that the steps of the walk are of the same size. If successive steps are represented by R_j , then the mean square displacement of a random walk is given by

$$\langle \zeta_k^2 \rangle = \sum_{j=1}^k \sum_{i=1}^k \langle R_j \cdot R_i \rangle = k A(j, i), \quad (1.36)$$

with a correlation function defined as $A(j, i) = \langle R_j \cdot R_i \rangle / |R|^2$. The probability for the end-to-end vector being of magnitude lying in the range $(\zeta, \zeta + d\zeta)$, equivalently, of lying in a shell of radius ζ and thickness $d\zeta$, is given by

$$P_k(\zeta) d\zeta = 4\pi\zeta^2 p_k(\zeta) d\zeta, \quad (1.37)$$

subject to the normalizing condition that

$$\int_0^{\zeta_{\text{fix}}(k)} P_k(\zeta) d\zeta = \int_0^{\zeta_{\text{fix}}(k)} 4\pi\zeta^2 p_k(\zeta) d\zeta = 1, \quad (1.38)$$

where $P_k(\zeta)$ is a density function for the random variable, ζ and $p_k(\zeta)$ is a density function relating to spherical shells. In Equation 1.37, $P_k(\zeta)$ is related to the function $\Phi_k(v_1, \dots, v_k)$ by

$$P_k(\zeta) = \int_{|v_1 + \dots + v_k|=\zeta} \Phi(v_1, \dots, v_k) dv_1 \dots dv_k. \quad (1.39)$$

Well-known solutions to Equation 1.37 exist for random unrestricted walks. However, as the spheres are non-intersecting, the consecutive steps are subject to condition (3.1.2), leading to self-avoiding random walks (SARWs). Furthermore, the SARWs are limited by the finite space around the sphere's surface. We have shown earlier by geometrical calculations that the maximum end-to-end distance, that is the asymptotic limit for such SARWs decreases towards zero for $k \rightarrow 12$. The additional fixed sphere requirement limits the configurations of each cluster for $4 \leq k \leq 6$, such that ζ_{max} cannot be reached and must be replaced by $\zeta_{\text{max}}^{\text{fixed}} \leq \zeta_{\text{max}}$. We note that $\zeta_{\text{max}}^{\text{fixed}} = \zeta_{\text{max}}$ for $k = 7$ to 12. There is approximate symmetry in the values of ζ_{max} with respect to $k = 6$ and in the values of $\zeta_{\text{max}}^{\text{fixed}}$ with respect to $k = 7$.

The function $P_k(\zeta)$ assumes a special and unique form for all clusters ($k = 4 \dots 12$) for which $\zeta = 0$. For example, for equidistant angular configurations of points, $P_k(\zeta = 0) = 1$ by definition. Furthermore, clusters derived from Bravais lattices with $k = 6, 8$, and 12 (a subset of clusters with equidistant configurations) also have $\zeta = 0$, and $P_k(\zeta) = 1$.

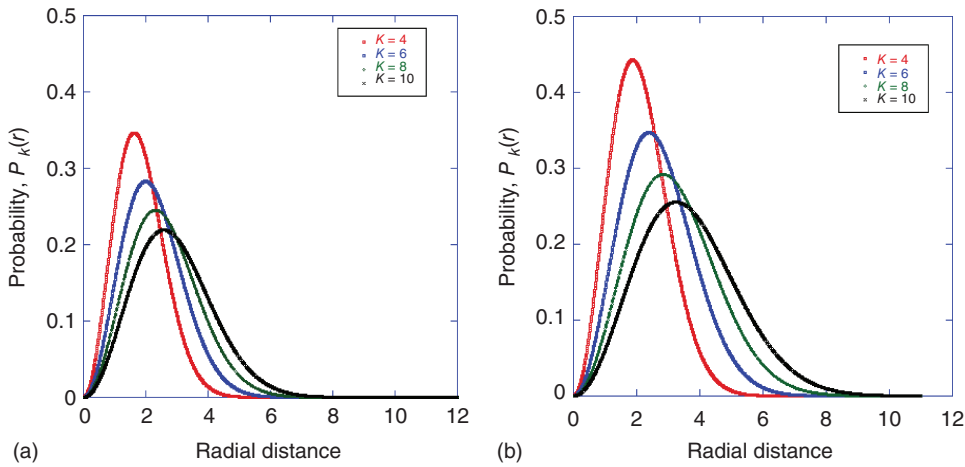


Figure 1.22 Probability functions for the random variable, ζ , for clusters with the values of k as shown. (a) Gaussian random walk and (b) self-avoiding random walk. In the latter case, peaks for SARW occur at larger values of k .

Table 1.6 Most probable random walk distances from Figure (1.22)

k	Gaussian	SARW	Ratio of SARW/Gauss
4	1.64	1.87	1.14
6	2.00	2.40	1.20
8	2.33	2.87	1.23
10	2.60	3.27	1.25

Therefore, for all regular clusters, $\zeta = 0$. For irregular clusters $\zeta \geq 0$, and the probability function, $0 \leq P_k(\zeta) < 1$. The variation of $P_k(\zeta)$ with k for irregular clusters is shown for GWR and SARW in Figure 1.22. The peak positions for the probabilities as a function of k have been determined from the graphs and are given in Table 1.6. The data shows how the end-to-end distance increases with k for the SARW relative to the Gaussian walk.

1.3.4.4 Physical Meaning of the Closing Vector, ζ

The geometry of an irregular cluster is adequately specified by the coordination number, k , and the magnitude of the closing vector, ζ . As stated before, the orientation of the cluster in space is not important, unless the cluster is placed in a physical force field, which may be magnetic, electric, elastic, or of any other nature. Then, the field will interact with the cluster through its geometrical and constitutional properties. The strength and direction of the interaction will be in proportion to the magnitude and direction of the closing vector, ζ .

Consider calculating a physical property of individual clusters. Let the vector polygon of Equation 1.29 be a piece-wise smooth curve C in \mathcal{R}^3 . Let \vec{p}_j be the

polarity vector associated with each pair of spheres in the cluster identified with the radial vector, \vec{R}_j , that is the polarity of a pair comprising the inner and one outer sphere. Then, the polarity of the cluster is simply,

$$\vec{p}_{\text{cluster}} = \sum \vec{p}_j = c \times \sum_{j=1}^{\kappa(x_\ell)} \vec{R}_j = c \times \vec{\zeta}, \quad (1.40)$$

where c is a material characteristic constant. Let a charge of q Coulombs be associated with each pair of spheres. Then, the cluster placed in an electric field \vec{E} experiences a force acting on it that can be calculated using Green's Theorem:

$$\vec{F} = \oint_C \vec{E}(x) \cdot d\vec{p}(x) \quad (1.41)$$

In materials science, the *coercivity* (also called the *coercive field* or *coercive force*) of a ferromagnetic material is the intensity of the applied magnetic field required to reduce the magnetization of that material to zero after the magnetization of the sample has been driven to saturation. Materials with high coercivity are called *hard ferromagnetic materials* and are used to make permanent magnets. Permanent magnets find application in electric motors, magnetic recording media (e.g. hard drives, floppy disks or magnetic tape) and magnetic separation. A material with a low coercivity is said to be soft and may be used in microwave devices, magnetic shielding, transformers or recording heads.

Other physical and mechanical properties can be related to the ζ function in a similar way.

1.3.4.5 Spherical Harmonics

Another way to describe the configuration of a cluster is by means of spherical harmonics, for which a general equation is as follows:

$$g_{\mu,\nu}(\phi, \theta) = \sum_{l=0}^L \sum_{m=-l}^l a_l^m(\mu\nu) Y_l^m(\phi, \theta) \quad (1.42)$$

where $a_l^m(i,j)$ are the spherical harmonics coefficients and $Y_l^m(\phi, \theta)$ are corresponding Bessel functions.

Spherical harmonics is an extension of Fourier series into three dimensions in spherical coordinates. The trigonometric functions in two dimensions represent the fundamental modes of a vibrating string, the spherical harmonics represent the fundamental modes of vibration of a sphere in much the same way. Fourier series decomposes periodic functions into the sum of simple oscillating functions, that is sines and cosines (or complex exponentials), and equivalent summation applies to spherical harmonics, as can be seen from Equation 1.42.

Wieder and Fuess (1997) proposed a modified Debye equation to consider the local structural order as follows:

$$I(\theta) = \sum_{i=1}^N \sum_{j=1}^N f_i f_j \left(\frac{n_{ij}}{d_{ij}} \right), \quad (1.43)$$

where:

$$n_{ij} = \int_{\phi=0}^{2\pi} \int_{\theta=0}^{\theta=\pi} \exp(i2\pi\mathbf{s}(\alpha, \beta, \theta) \cdot \mathbf{r}_{ij}(\phi, \theta)) \cdot h_{ij}(\phi, \theta) \sin \theta d\theta d\phi \quad (1.44)$$

$$d_{ij} = \int_{\phi=0}^{2\pi} \int_{\theta=0}^{\theta=\pi} h_{ij}(\phi, \theta) \sin \theta d\theta d\phi. \quad (1.45)$$

It can be noted that for $h_{ij}(\phi, \theta) = 1$, that is for spherical symmetry, the original Debye scattering Equation 1.42 is recovered. For the case, $h_{ij}(\phi, \theta) \neq 1$, the orientation function can be expressed in terms of spherical harmonics:

$$h_{ij}(\phi, \theta) = \sum_{\ell=0}^L \sum_{m=-\ell}^{+\ell} a_{\ell}^m(i, j) Y_{\ell}^m(\phi, \theta) \quad (1.46)$$

The probability function, $P(k)$ of Equation 1.37, has both a descriptive character and a predictive role. It describes the distribution of configurations for all clusters, as well as indicating the most probable configuration for each cluster. In that sense, it is also more appropriate for describing configurations of random clusters in ideal amorphous solids than spherical harmonics. The Q6 component of spherical harmonics has a range of different values for regular configurations, but it gives a non-discriminating value of zero for random packings. Only two-dimensional plots of spherical harmonics differentiate between various configurations. The function, $P(k)$, however, gives a more comprehensive statistical description of the range of random configurations around the most probable arrangement with a clear differentiation between clusters with different coordinations (k values) and independent of the choice of frame of reference.

1.4

Geometry of Sphere Packings

Packing of spheres is an assemblage (aggregate) of spheres of either finite or infinite extent. It is an object that can be studied *per se* in terms of its geometry and mathematical properties, and also it is a useful model of atomic arrangements in solids and liquids. The packing is a created object, that is either imagined or physically put together in some manner. This can be done in one two ways:

- by following a strict rule (or a set of self-consistent rules),
- in an undefined, or only partially defined way.

Packings in the second category are typically those based on so-called random pouring of spheres into containers and any variations thereof or on molecular dynamics computations. These methods simulate structures that resemble those of real solids, with particular packing arrangements and imperfections not present in perfect solids which are free of any imperfections by definition. Such models are ubiquitous and will be considered later.

Models in the first category are deterministic. If the geometrical rule of packing and the size of the spheres are known, then the packing can be created repeatedly

and reproducibly following the rule, always with the same predictable result. This means that the created packing is repeatable and verifiable, which is a requirement for modelling of ideal structures, such as crystalline, quasi-crystalline and ideal amorphous atomic arrangements.

Packing of spheres involves a volume, V containing N number of hard spheres. For simplicity, assume all spheres to have the same diameter. The number density of such an assembly is,

$$\rho = N/V. \quad (1.47)$$

The total volume can be divided into

- volume occupied by all spheres, $V_o = N \cdot (4/3)\pi r^3 < V$
- unoccupied volume, $V_u = 1 - V_o$.

Naturally, for $N = 0$, $V_o = 0$, $V_u = V$ and $\rho = 0$. As N increases, the number density and the corresponding volume fraction, $0 \leq V_o/V < 1$, increases simultaneously. Under the condition of sphere impenetrability, the volume fraction is always less than one.

The maximum value of the volume fraction depends on both the arrangement of the spheres and the shape of the volume V . If the volume is concave at all points of its surface, and if the number of spheres that are packed into it is sufficiently large, the effect of its shape becomes negligible. Then, the geometrical arrangement of the spheres is the only deciding factor with regard to the maximum numerical density or volume fraction. The largest value of the volume fraction is found in sphere packings representing hexagonal close packed or fcc crystallographic arrangements. Any other arrangements result in lower maximum packing fractions, as described in the following.

We use a symbolic notation for a general packing of spheres. Let S_a represent a sphere of diameter, a , and let Ω be a set of points in Cartesian space representing the centres of N such spheres,

$$\Omega = \{x_1, x_2, \dots, x_N\}. \quad (1.48)$$

Then,

$$S_a + \Omega \quad (1.49)$$

is a packing of spheres.

We first note some general properties:

- 1) Scale invariance:
if $S_a + \Omega$ is a packing, then so is $S_{ca} + c\Omega$ for every positive c .
- 2) Homogeneity of point field:

Let $N = [xn]$ be a point field. The point field is homogeneous if $N = [xn]$ and $N = [xn + x]$ have the same distribution for all $x \in E_n$. Then the density is independent of position and selection of the field. Therefore, packing fraction should be the same regardless of variation in atomic sizes in multi-atomic glassy alloys, that is random packing independent of the size of Voronoi cells.

1.4.1

Fixed and Loose Packings

Consider a cluster of spheres in packing comprising one inner sphere in the centre and k -number of outer spheres touching it. The number and arrangement of the outer spheres define a fundamental characteristic of the inner sphere in such a cluster; it can be in one of two distinctly different arrangements:

- Fixed spheres packing - A sphere is in a *fixed* position, when, for $4 \leq k \leq 9$, no more than $(k - 1)$ of the outer spheres are located on one hemisphere; for $k > 9$, the sphere is always in a fixed immovable position. This condition implies that the touching spheres form a cage around the inner sphere. In \mathbb{R}^3 , a minimum of four outer spheres is needed to fix the inner sphere. Otherwise, the inner sphere is *loose* and can move (Stachurski, 2003).
- Loose spheres packing - A sphere is always in a *loose* position, when, for $4 \leq k \leq 9$, all contacts are on one hemisphere only; the sphere may be confined but it is not fixed and can move to other loose positions in its vicinity. A packing containing loose spheres is called *loose packing*.

Any arrangement of outer spheres on a cluster with $k < 4$ cannot form a locking cage around the inner sphere, which gives reason to the lower limiting value, $k_{\min} = 4$, of touching neighbours in arrangements of spheres guaranteed to represent a perfect solid body. A perfect solid body is one in which all spheres are in fixed positions, disallowing any translational movement of any sphere. Frictionless rotations are allowed as they have no effect on solidity.

We shall now consider three types of packings, distinguished entirely by the geometrical arrangement of the spheres.

1.4.2

Ordered Packing

For ordered (crystalline) packing, the set containing the coordinates of the sphere centres possesses translational regularity in their values, and therefore, the position of every sphere in the ordered structure can be predicted using the formula:

$$\vec{r}_{\text{sphere}} = S(r_0) + u \cdot \vec{a} + v \cdot \vec{b} + w \cdot \vec{c} \quad (1.50)$$

If $\vec{a}, \vec{b}, \vec{c}$ are linearly independent vectors in Cartesian space, then the set,

$$\Lambda = \left\{ \sum_{i=1}^3 z_i \vec{a}_i : z_i \in \mathbb{Z} \right\} \quad (1.51)$$

is called a *lattice*, where \mathbb{Z} is a set of all integers (\mathbb{Z} is from German ‘Zahlen’ meaning numbers), and $(\vec{a}, \vec{b}, \vec{c})$ is the basis for Λ .

We call

$$S_a + \Lambda \quad (1.52)$$

an ordered (translative) packing of S_a on the lattice Λ , if

$$(\text{int}(S_a) + \mathbf{x}_1) \cap (\text{int}(S_a) + \mathbf{x}_2) = \emptyset, \quad (1.53)$$

whenever \mathbf{x}_1 and \mathbf{x}_2 are distinct points in Λ . In the theory of crystallography, there are 14 distinct Λ -sets corresponding to 14 Bravais crystal lattices.

Ordered packing of spheres is evidenced by regularity of the arrangement. The most direct evidence is provided by testing for elements of symmetry displayed by the set. In particular, one can imagine a plane passing through such a packing on which many of the sphere's centres lie in some arranged ordered pattern. There is always an imaginary plane, passing through the set, which contains a large subset (more than three) of the points. This is the basis for crystallographic (translational) and for quasi-crystalline patterns (rotational regularity in the latter case).

We now require some special properties of the set Λ :

- 1) For any point, $x_\ell \in \Lambda$, its nearest neighbours are always equidistant from that point, that is $|x_{\ell j} - x_\ell| = a$ for $j = 1, \dots, \kappa(x_\ell)$, where $\kappa(x_\ell)$ is the number of nearest neighbours. *This requirement implies that spheres are non-intersecting, that all spheres have the same diameter, and that nearest neighbours are touching.*
- 2) The number of nearest neighbours, $\kappa(x_\ell)$, is bounded: $[4 \leq \kappa(x_\ell) \leq 12]$. The lower limit of 4 is imposed by the condition that all spheres are fixed, and the upper limit of 12 is established as an absolute limit by the Kepler theorem.

1.4.3

Disordered Packing

Degree of disorder is defined by physicists and materials scientists as follows: Let p be the probability that a lattice position is occupied by a foreign replacement. The degree of disorder is expressed as

$$\begin{aligned} D &= \frac{\text{actual value of } p - \text{value of } p \text{ for complete disorder}}{\text{value of } p \text{ for complete disorder} - \text{value of } p \text{ for complete order}} \\ &= \frac{p - r}{1 - r} \end{aligned} \quad (1.54)$$

When order is complete, p is unity and D is therefore unity. When disorder is complete (whatever that means) and the arrangement of replacements quite random, only a fraction of r of the replacements will be in the positions of order. Therefore $p = r$, and $D = 0$.

This packing implies that it is disordered from the regular packing (by the introduction of imperfections usually referred to in crystallography as defects). Since in principle disorder can be reversed, disordered packing is deemed to be structurally derived from the ordered packing and therefore different from random packing.

1.4.4

Random Packing

We note that a random process is a repeating process whose outcomes follow no describable deterministic pattern but follow a probability distribution.

There exist three mechanisms responsible for random behaviour in systems:

- 1) Randomness coming from the initial conditions (chaos). Example: the motion of the end point of the so-called double pendulum is chaotic.
- 2) Randomness coming from the environment (Brownian motion). Example: (a) the motion of a gas molecule or (b) the tossing of a coin.
- 3) Randomness intrinsically generated by the system. Typically shows statistical randomness whilst being generated by an entirely deterministic causal process. This is also called *pseudo-randomness*. Example: (a) generation of random numbers by computer and (b) random packing of spheres.

The formation of real amorphous materials comes from randomness of density fluctuations in the liquid (Brownian motions). However, the construction of a random packing of spheres is generated by rules, and therefore, it is a pseudo-random process.

Random packing is fundamentally different from crystalline and quasi-crystalline packing and also different from disordered packing, and we represent it symbolically by the notation:

$$S_a + X \quad (1.55)$$

Random packing is characterized by irregularity of *all* point-to-point distances in the set X . An algorithmically random sequence (or random sequence) is an infinite sequence of binary digits that appears random to any algorithm. The definition applies equally well to sequences on any finite set of characters. The positions of the sphere centres cannot be described by an equation of the type (Equation 1.50). Instead, the distances between the points are described by an appropriate statistical density distribution function.

1.4.5

Random Sequential Addition of Hard Spheres

Consider a volume, V , into which hard spheres of the same diameter, d , are added sequentially, one at a time. The placing of each sphere inside the volume is at randomly chosen positions, with the constraint that spheres must not overlap (consequently, each addition must be preceded by a test of the available space). At any stage of this process, the packing is described by,

$$S_a + X_{RSA}. \quad (1.56)$$

If random sequential addition (RSA) of spheres always starts with V empty, and if it is repeated with ever-increasing V , and stopped when the same average density ρ is achieved, then in the limit $N, V \rightarrow \infty$ there is a unique limiting density, ρ^* ,

called the *saturation density*. With random sequential addition, it is obvious that a saturation density ρ^* is always less than the highest density of the ordered packing.

The process of random sequential packing can be described as follows. Let $v_{\text{ex}} = (4/3)\pi d^3$ be the volume from which one sphere excludes the center of another. Let $w_{\text{ex}} = w(\mathbf{r}_1, \mathbf{r}_2)$ be the combined volume from which the center of a third sphere is excluded by two spheres, one centred at \mathbf{r}_1 and the other at \mathbf{r}_2 . We note that w_{ex} is not constant but varies from a minimum value of $(19/12)\pi d^3$ when the volumes, v_{ex} , overlap at $|\mathbf{r}_1 - \mathbf{r}_2| = d$ to a maximum value of $(8/3)\pi d^3$ when the centres of the two spheres are sufficiently far apart, $|\mathbf{r}_1 - \mathbf{r}_2| \geq 2d$.

Let $\mathbf{r}_1, \mathbf{r}_2, \mathbf{r}_3$ be an allowable configuration of the centres of the three spheres with the probability,

$$P(\mathbf{r}_1, \mathbf{r}_2, \mathbf{r}_3) dv_1 dv_2 dv_3 \quad (1.57)$$

where one of the spheres has its center in the infinitesimal volume element dv_1 at \mathbf{r}_1 , one in dv_2 at \mathbf{r}_2 and one in dv_3 at \mathbf{r}_3 . Then, from the definition of random sequential addition,

$$P(\mathbf{r}_1, \mathbf{r}_2, \mathbf{r}_3) = 2V^{-1}(V - v_{\text{ex}})^{-1}[(V - w_{12})^{-1} + (V - w_{23})^{-1} + (V - w_{31})^{-1}] \quad (1.58)$$

where $w_{ij} = w(\mathbf{r}_i, \mathbf{r}_j)$.

This probability density is not uniform in the space of allowable configurations but depends on the configuration through the w_{ij} 's. The greater the extent to which the exclusion volumes associated with the spheres i and j overlap, the smaller are w_{ij} and $(V - w_{ij})^{-1}$, and also the smaller is P . Thus, the probability, P , is biased in favour of those triplet configurations in which pairs of spheres are so distant that their associated exclusion spheres do not overlap.

By contrast, a uniform probability density in the space of allowable configurations, such as would characterize an equilibrium distribution, would for this case of three spheres be given by,

$$P = 6V^{-1}(V - v_{\text{ex}})^{-1}(V - \langle w_{ij} \rangle)^{-1}, \quad (1.59)$$

where

$$\langle w \rangle = (V - \omega)^{-1} \int w_{12} dv_2 \quad (1.60)$$

the integration being extended over all positions \mathbf{r}_2 in V of the center of a second sphere, which are allowed when a first sphere is fixed with its centre at \mathbf{r}_1 . The constant $\langle w \rangle$ and the functions w_{ij} may be readily expressed in terms of the sphere diameter d , but this is not pursued here.

Sequential addition produces a configuration in which there remain no gaps as large as the sphere diameter, and there need not be any spheres in contact in this configuration. It belongs to the loose spheres packing category. Sequential random addition can be considered as an approximation to the equilibrium distribution in a model of hard sphere fluid.

1.4.6

Random Closed Packing of Spheres

Closed packing belongs to the fixed spheres packing category. The essential element of this random closed packing is that each new sphere that is added must rest on three, and only three spheres that have unequal spacings between them, $BC \neq CD \neq DB$, as shown in Figure 1.23.

In any group of four nearest-neighbour spheres selected from such a packing, the centres of three non-touching spheres must form an irregular triangle, as shown in Figure 1.23. The sphere, A, is touching the three spheres, B,C,D, to form touching contacts. Each triangle, ADC, ADB and ABC, is an isosceles triangle but with different angles: $\angle DAC \neq \angle CAB \neq \angle BAD$.

It is recalled from Section 1.3 that irregular clusters, constructed by the Fürth method or by the blocking method, consists of one inner sphere and k outer spheres randomly positioned. The outer spheres provide $k + 2$ sites for the addition of spheres, which satisfy the condition for any combination of its three adjacent spheres that,

$$(\text{two sphere diameters}) > DC > DB > BC > (\text{one sphere diameter})$$

Now, consider an irregular cluster such as shown in Figure 1.24. Any three adjacent outer spheres provide a site for addition of another sphere. The added sphere, together with the underlying three spheres, forms a group of four spheres similar to that described earlier and depicted in Figure 1.23. Such addition of spheres onto available three-sphere sites will result in growth of the cluster. At the completion of the first growth stage, the original cluster will be increased in size by the addition of the second layer of spheres. All spheres in the second layer will have unequal distances between them and from the central inner sphere.

Next, the process of identifying and filling in of the possible sites can be repeated again, and again, according to the rules listed in the following. The above-mentioned process can be applied for as many times as required, until the

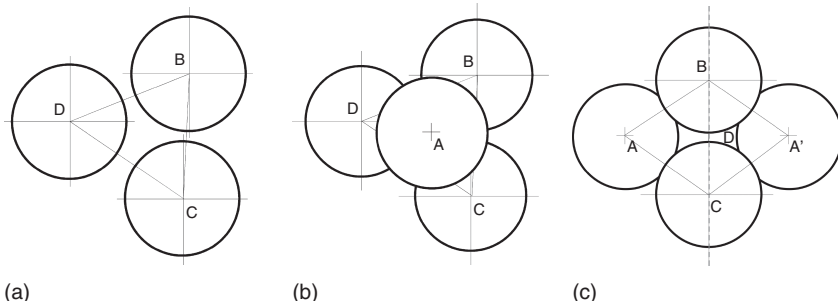


Figure 1.23 (a) Equal size spheres B, C and D, separated by unequal distances ($DC > DB > BC$), forming an irregular triangle. (b) Sphere A touches each of the underlying

spheres B, C and D, and therefore, its centre is equidistant from each. (c) A five sphere subcluster; plane passing through BCD is a plane of mirror symmetry.

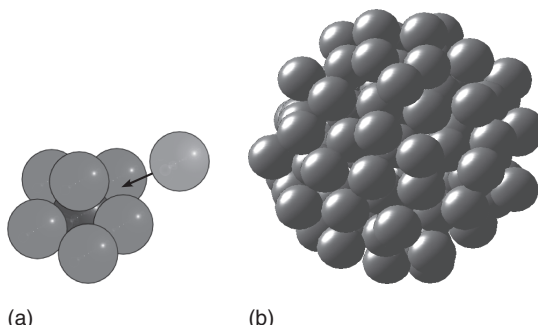


Figure 1.24 (a) A primary cluster with a sphere added to a triangular site of an irregular shape formed by three adjacent outer spheres. (b) A cluster with several layers of spheres, added by the same method.

desired size of the cluster is reached. The geometrical construction follows a set of rules so that the outcomes are always reproducible and verifiable.

Rules for sphere addition to $S_a + X_{RCP}$ packing

- 1) For a given cluster of spheres, identify and index all possible triangular sites on its surface, based on three adjacent non-touching spheres.
 - 2) Find (compute) the centres for spheres that can be potentially added to the sites
 - 3) Sort all sites in order from the closest to the furthest in terms of the distance to the centre of the inner sphere;
 - 4) Add a sphere to the site of the closest distance and then add a sphere to the next site in terms of the closest distance from the centre;
 - 5) Ascertain that the second sphere does not overlap; reject the second sphere if there is an overlap; and
 - 6) Continue the process (steps 4–5) until all allowable sites are filled in (with every completion of the loop another coordination shell is added).

This packing of spheres is represented by the notation:

$$S_a + X_{RCP} \quad (1.61)$$

This is a pseudo-random packing because it always results in the same packing, that is the same set X_{RCP} for the same initial configuration of the random cluster. However, the positions of the spheres are randomly distributed in space, without any short-, medium- or long-range order. Furthermore, the packing is different (different sphere positions) if the initial configuration of the random cluster is different. The random close packing possesses the following properties:

- 1) *The hard sphere condition* (Section 1.2); if x_i and x_j are the coordinates of two adjacent spheres, the $(x_i^2 - x_j^2)^{1/2} \geq D$ is true for all spheres without exception.
 - 2) *The fixed sphere requirements* (Section 1.3); all spheres are in fixed positions.

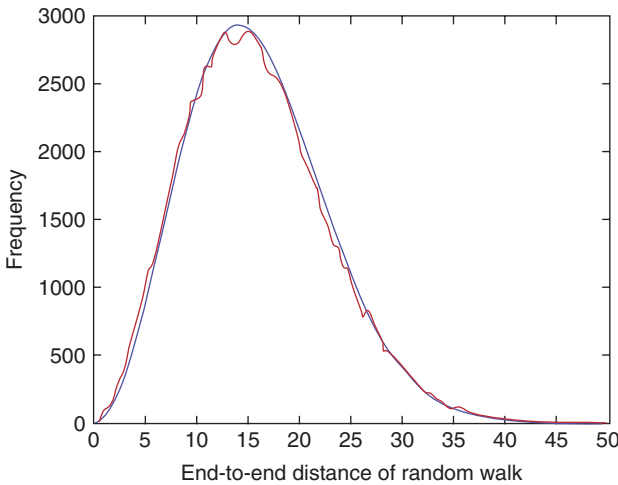


Figure 1.25 Probability distribution for random walks along contacting spheres in a random packing. The dithering curve is from experimental results, the smooth curve

corresponds to theoretical Gaussian distribution. The agreement between the two curves is very close.

- 3) *Isotropy of a point field*; If $R(\theta)$ represents rotational transformation, and if $N = xn$ and $R(\theta)N = R(\theta)xn$ have the same distribution for any angle θ , then the field is said to be isotropic.
- 4) *Motion invariance*; If a field is isotropic and homogeneous, then it is said to be motion invariant.

In Section 1.3, radial vectors emanating from the centres of all spheres to the contact points on their surfaces were defined. The construction, when carried out for all spheres in a packing, results in a three-dimensional network spanning the whole body. The sum of all vectors in all spheres must tend to zero as the size of the body increases to infinity:

$$\sum_{i=1}^N \vec{R} \rightarrow 0, \quad \text{as } N \rightarrow \infty, \quad \text{summation over all vectors} \quad (1.62)$$

proof: $\sum \vec{R} = \sum \langle R \cos \Theta \rangle = R \sum \langle \cos \Theta \rangle = 0$. For a finite system (Equation 1.62) becomes $\sum \vec{R} \rightarrow 0$ as $N \rightarrow \infty$.

A large simulation cell with more than 2×10^6 spheres, comprising approximately 60 coordination shells, was used for random walk experiments. Random walks of 300 steps were carried out from one touching sphere to another touching sphere. No limitations imposed by the cell boundary were encountered. All random walks were started at random from the innermost 10^4 spheres. To obtain reasonable statistical distribution, 10^5 such random walks were executed, with the result shown in Figure 1.25. The wavering curve represents the experimentally determined distribution; the smooth curve is drawn in accordance with Gaussian statistics of random walk (Equation 1.39). The agreement is remarkably good,

confirming that the size of the cell is sufficient to carry out undisturbed random walks along the spheres. However, the random walk element, although necessary to identify this type of amorphous solid, is not a measure sensitive enough to detect the presence of packing imperfections, and therefore not sensitive enough to distinguish ideal amorphous solids from non-ideal amorphous solids.

Random walks and Markov chains

A Markov chain is a stochastic process with the Markov property on a finite or countable state space. The term *Markov chain* refers to the sequence (or chain) of states such a process moves through. Usually, a Markov chain is defined for a discrete set of times (i.e. a discrete-time Markov chain).

Often, random walks are assumed to be Markov chains. A discrete-time random process involves a system which is in a certain state at each step, with the state changing randomly between steps. The steps are often thought of as moments in time, but they can refer to physical distance or any other discrete measurement; formally, the steps are the integers or natural numbers, and the random process is a mapping of these two states. The Markov property states that the conditional probability distribution for the system at the next step (and in fact at all future steps) depends only on the current state of the system and not additionally on the state of the system at previous steps.

1.4.7

Neighbours by Voronoi Tessellation

Now, we can increase the size of the primitive cluster to include additional layers of spheres around it, as shown schematically by the circles for two dimensions in Figure 1.26, and consider neighbours of the A sphere.

We assign spheres into discrete neighbouring positions by the Voronoi tessellation method when they do not touch the inner central sphere. This method is used to allocate spheres into the so-called *nearest neighbours* (touching and not touching the inner sphere) and to separate them from further positioned,

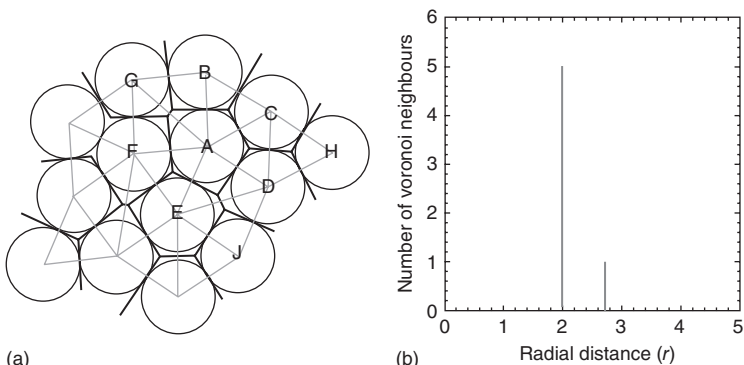


Figure 1.26 (a) A cluster of circles and construction of Voronoi polygons around circles in two dimensions. (b) Histogram of Voronoi nearest neighbours around circle A.

more distant neighbours. In this method, a Voronoi polyhedron is constructed for each sphere according to a unique mathematical procedure (Voronoi, 1908; Brostow *et al.*, 1978; Tsumuraya *et al.*, 1993). Then, by definition, two spheres are Voronoi neighbours if they share a common face of their respective polyhedra.

Formally, the Dirichlet–Voronoi polyhedron is constructed around each sphere by space partition, as defined in the following equation:

$$V_V(x_{ij}) = \{x : \|x, x_i\| \leq \|x, x_j\| \text{ for all } x_j \in X_{IAS}\} \quad (1.63)$$

For the present purposes, we give an operational definition, and for perspicuity, we limit it to two dimensions. Consider a set of points, each representing centres of circles (Figure 1.26). First, we draw links between neighbouring points. Then we take each link and produce a line perpendicular to it and passing through the point equidistant from terminal points. Such bisectors produce polygons around the points. For each point, the smallest polygon so constructed is the Voronoi polygon. It delineates the space that belongs to that particle. Extension to three dimensions is straightforward, in which polygons become polyhedra. The number of faces of a Voronoi polyhedron is equal to the number of all h -neighbours.

One can always, in an unambiguous way, divide up a structure, made of points, into (usually irregular) tetrahedra. This is done using first the Voronoi (or Dirichlet) decomposition of space into individual cells which contain the regions of space, closer to a given point than to any other one. In generic cases, the Voronoi cells have three faces sharing a vertex of the cell. Then, connecting the original points of the set whenever their associated Voronoi cells share a face, defines a unique decomposition of the space into tetrahedra. This simplicial decomposition is equivalent, in three dimensions, to a point set triangulation in two dimensions. This procedure also provides the best way to define the coordination number in dense structure: it is equal to the number of faces of the Voronoi cell. In a topological sense, the Voronoi cell and the coordination polyhedra are dual. In a tetrahedral division of space, the set of vertices closest to a given site forms its first coordination shell, which is a triangulated polyhedron (a deltahedron).

According to Figure 1.26a, circles B to F are the Voronoi coordination shell neighbours to sphere A (by touching) and circle G is also a neighbour, although not touching. Spheres H and J are not Voronoi neighbours; they do not share a common face with A. The criterion for the first Voronoi coordination neighbour is that the distance between centres is within the range: $D \leq h \leq D\sqrt{2}$. In three dimensions, the criterion is $D \leq h \leq D\sqrt{8/3} = 1.633 D$ (Lee *et al.*, 2010). Faces tangential to the sphere/circle separate D -neighbours and contain respective contact points. Therefore, the Voronoi tessellation method allows a greater number of spheres to be nearest neighbours than just the touching neighbours—significantly so for three-dimensional clusters. This is clearly evident in Figure 1.27b which shows the distributions for both touching and Voronoi nearest neighbours obtained from a random packing of spheres of the same size.

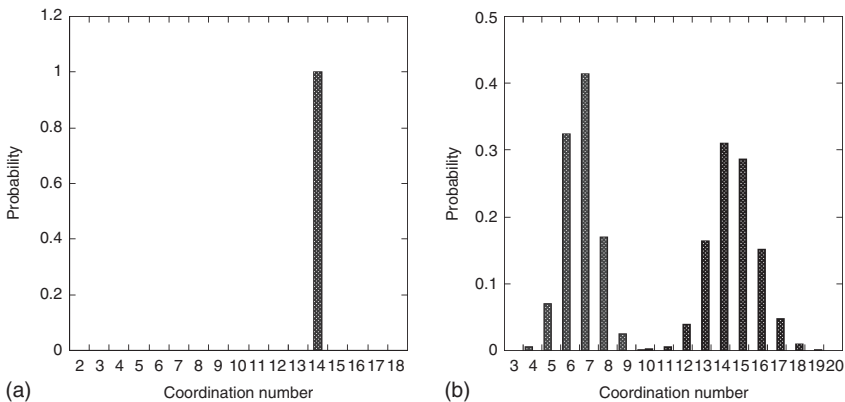


Figure 1.27 Histograms of neighbours according to Voronoi method: (a) ordered (bcc) cluster and (b) statistics for random clusters with touching neighbours (on left) and Voronoi neighbours (on right).

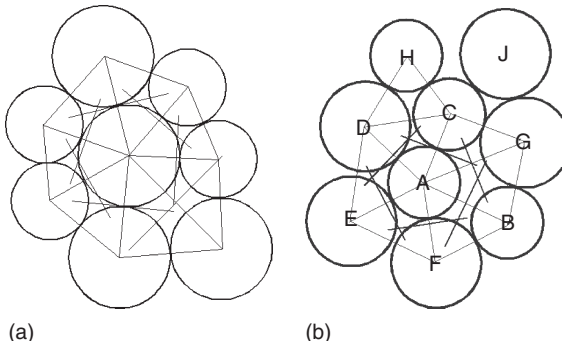


Figure 1.28 Voronoi tessellation applied to a cluster with two sizes of spheres. Notice that the bisectors between large and small spheres fall within the larger sphere: (a) large inner spheres and (b) small inner sphere.

For disordered, irregular and random packing, the Voronoi polyhedra are irregular and vary in size and shape. For regular clusters and ordered packings, particularly on Bravais lattices, each Voronoi polyhedron is the same size and shape for each and every sphere (of the same size). Thus, the coordination number distributions, as seen in Figure 1.27b for the random packing, degenerate into a single valued function for ordered clusters. For example, for a bcc structure every primary cluster has 8 touching neighbours plus 6 Voronoi neighbours, giving all together 14 Voronoi nearest neighbours, as seen in Figure 1.27a. Crystallographers use the term *Wigner-Seitz cells* for the Voronoi construction (Wigner and Seitz, 1933).

Voronoi tessellation does not work straightforwardly for spheres of different sizes. This is clear from the diagrams shown in Figure 1.28, where it can be observed that the bisector lines do not go through the contact points, but cut into



Figure 1.29 Hryhoryi (Georgyi) Voronoi, Ukrainian mathematician (1868–1908) (from Wikipedia).

the larger sphere. The problem does not present itself in cases where packing simulation is carried out by molecular dynamics. In such cases, atoms are force centres and not spheres with clearly defined radii; and therefore, unwittingly, the problem is neglected. Consequently, what are nearest neighbours by this method for multi-sized spheres has to be redefined and weighted Voronoi tessellation applied.

Hryhoryi Voronoi, Ukrainian mathematician whose portrait is shown in Figure 1.29 (1868–1908). A conference dedicated to Voronoi diagrams is held every two years and published in the International Journal of Voronoi Diagram Research Center, Hanyang University, Seoul, Korea.

The mathematics of the polyhedra in question begins with the work of Johann Peter Dirichlet (Dirichlet, 1850), followed by the work of Gregoryi (pronounced Hrehoryi) Voronoi, an Ukrainian mathematician, who was a student of A. Markov (of Markov chains) in Kiev, later working in Warsaw in the beginning of the twentieth century (Voronoi, 1908, 1909). This is why the polyhedra are most often named after him.

The application of Voronoi tessellation to describe the amorphous structures can be traced to the early work by Bernal and his coworkers on the structure of liquids. One of the earliest publications of this type appeared in 1970 by Finney (1970a), in which early computations of Voronoi polyhedra were carried out on random close packed structures, using main-frame computers. The relationship between the distribution of Voronoi volumes and the radial distribution function was established for these simple monoatomic structures in a subsequent publication (Finney, 1970b).

Brostow *et al.* developed the first exact computational method of Voronoi tessellation (Brostow *et al.*, 1978). Definitions of indirect, degenerate and quasi-direct neighbours of a given particle (point) have been introduced at the same time. The method relies on constructing first the so-called direct polyhedra, relatively simple, with a considerable saving of time. Shortly after, Tanemura *et al.* (1983) published an efficient algorithm for computing the Voronoi tessellation, and these two papers must be considered to be the seminal works on this subject, including the definition of amorphous structure in solid materials and in liquids (Medvedev *et al.*, 1990).

The earliest Voronoi diagrams for polymers have been published by Theodorou and Suter (1985). The tessellation was computed for static, equilibrated structures, with the results describing mainly the Fürth distribution. Pfister and Stachurski

(2002) used the concept of Voronoi polyhedron around a polymer chain to postulate a deformation mechanism in amorphous polymers. For inorganic glasses, Voronoi tessellation approach was used by Tsumuraya and coworkers (1993). In addition, Watanabe and Tsumuraya (1987) studied liquid sodium by molecular dynamics and applied the Voronoi approach to distinguish glass formation from crystallization and in the distinction of amorphous solids and liquids.

The Voronoi diagram has also been used to define the fundamental difference between an amorphous solid and a liquid in terms of percolations of two kinds of structures (Medvedev *et al.*, 1990). Atomic level strain was connected to the Voronoi diagram (Mott *et al.*, 1992) and plasticity (Stachurski and Brostow, 2001).

It is important to stress that Voronoi polygons are an important concept in other branches of science, in particular that of surface visualization, as evidenced by two examples of publications by De Floriani *et al.* (1985), and Hoff *et al.*, (1999). The selected publications quoted here contain numerous references to other publications related to this topic.

Many computational packages have Voronoi routine built-in. For example, Materials Studio®, MatLab®, Mathematica®, Maple® and others.

1.4.8

Neighbours by Coordination Shell

A more general method for assigning spheres into positions relative to a central sphere is based on the radial distance from the centre. Given a central sphere (or a point), the number of spheres enclosed within each concentric shell, $r_{\text{shell}} \leq r \leq r_{\text{shell}} + dr$, represents the neighbours in that shell, as illustrated in Figure 1.30. In other words, the number of sphere centres in a shell of thickness, dr , at a distance, r_{shell} , from the origin is given by:

$$n(r) = \frac{N}{V} \int_{r_{\text{shell}}}^{r_{\text{shell}}+dr} g(r) 4\pi r^2 dr \quad (1.64)$$

where N represents the total number of spheres in the volume V extended over the whole body, and therefore, N/V is the numerical density of the body. The factor $4\pi r^2$ represents the surface area of the shell, and $g(r)$ is the *radial particle density distribution function*.

The radial density distribution function, frequently called the pair distribution function (PDF), describes the distribution of distances between pairs of particles contained within a given volume. Mathematically, if a and b are two particles in a fluid, the PDF of b with respect to a , denoted by $g_{ab}(\vec{r})$, is the probability of finding the particle b at the distance \vec{r} from a , with a taken as the origin of coordinates.

In statistical mechanics, the radial distribution function (or pair correlation function), $g(r)$ in a system of particles (atoms, molecules, colloids, etc.), describes how density varies as a function of distance from a reference particle. In simplest terms, it is a measure of the probability of finding a particle at a distance of r away from a given reference particle, relative to that for an ideal gas.

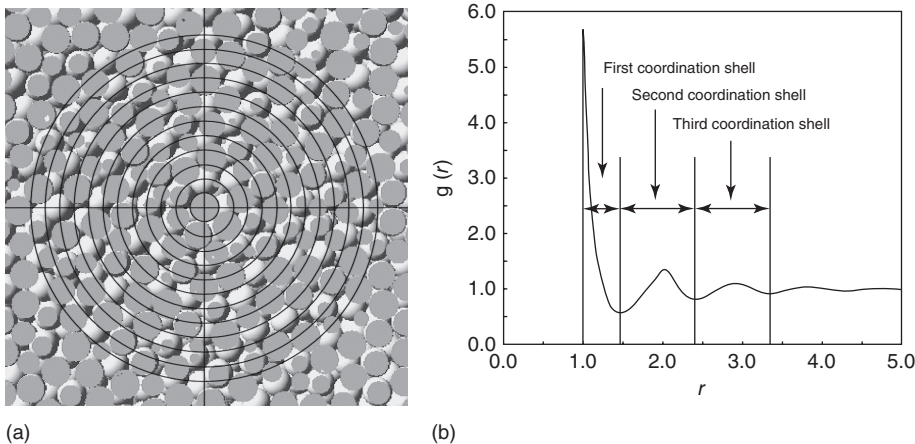


Figure 1.30 (a) Cross section through randomly packed spheres of the same size with concentric shells drawn in. (b) Radial distribution function for the packing on the left

plotted as a function of inter-sphere separation. The first three coordination shells are delineated by the vertical blue lines.

In computer simulations, the counting of individual spheres in a packing of spheres is made by means of the following formula, which is valid for any value of r :

$$g(r) = \frac{1}{\rho} \frac{n(\Delta r)}{4\pi r^2 \Delta r} \quad (1.65)$$

So derived $g(r)$ is a stepwise discrete function, although it is usually drawn as a smooth curve. It has a value of zero up to a distance $r_{\min} = 2R$ at which it rises sharply to a maximum value. For hard sphere packings, the initial slope at r_{\min} is infinity.

From its maximum value, the function decreases and oscillates, showing a number of peaks that diminish in height with increasing r . In the limit of $r \rightarrow \infty$, $g(r) \rightarrow 1$ because $n(r)/(4\pi r^2 \Delta r) \rightarrow \rho$ (Figure 1.30).

By this method, there will be first shell neighbours at distances corresponding to the first peak, second shell neighbours corresponding to the second peak, third shell neighbours and so on, as shown in Figure 1.30. Accordingly, the first coordination number is given by

$$n_1 = 4\pi\rho \int_{r_0}^{r_1} r^2 g(r) dr \quad (1.66)$$

The second coordination number is defined similarly:

$$n_2 = 4\pi\rho \int_{r_1}^{r_2} r^2 g(r) dr \quad (1.67)$$

We note that the smaller Δr in Equation 1.65 the finer the resolution of the PDF. This is clearly evident when comparing the PDFs in Figure 1.31a and b.

The initial slope of PDF ought to be vertical as in Figure 1.30. In Figure 1.31a, the slope is less than $+\infty$ because of the existence of the smaller spheres (atoms)

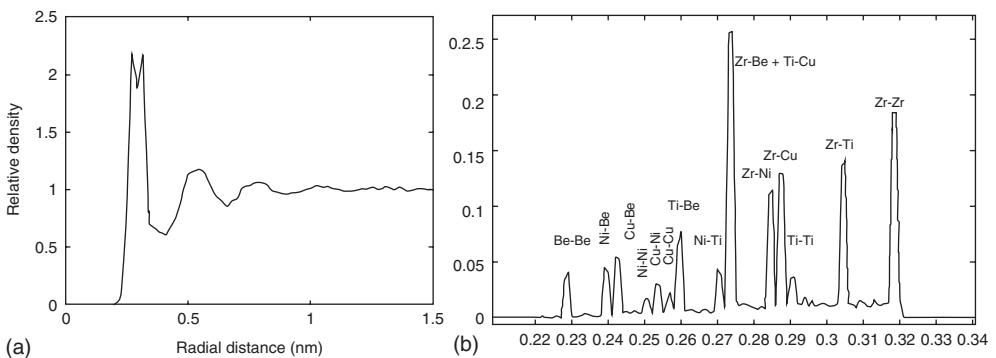


Figure 1.31 PDF for Zr-Ti-Cu-Ni-Be metallic glass computed using Equation 1.65. (a) With $\Delta r = 0.23$ nm and (b) with $\Delta r = 0.001$ nm. Note the change of horizontal scale.

at separation distances between 0.23 and 0.27 nm as seen in Figure 1.31b, whereas the double peak corresponds to the presence of Zr–Be and Ti–Cu pairs that happen to have the same separation. Indeed, Figure 1.31b shows the component peaks of the double peak in Figure 1.31a. All pairs under the first peak belong to the first coordination shell in accordance with the definition in Figure 1.30. All pairs under the second peak (between 0.33 and 0.70 nm) belong to the second coordination shell and so no.

1.4.8.1 Pair Distribution Function

The PDF describes the distribution of distances between pairs of particles. In relation to Figure 1.32, $g_{AB}(\vec{r})$ gives the probability of finding the particle B at a distance \vec{r} from particle A which is chosen to be at the origin. If the system of particles is homogeneous and isotropic, then there is an equal probability of finding particle B at any position \vec{r} , and the PDF becomes centre-symmetric, so that $p(\vec{r}) = 1/V$.

However, the probability of finding *pairs of particles* at given positions is not uniform. Then, the PDF is obtained by the two-body probability density function:

$$g(\vec{r}, \vec{r}) = p(\vec{r}, \vec{r}) V^2 \frac{N - 1}{N} \approx p(\vec{r}, \vec{r}) V^2 \quad (1.68)$$

For any particulate system, with N large enough to allow for a meaningful statistical analysis, $N - 1 \sim N$.

The simplest possible PDF for non-dense randomly packed spheres is

$$g(r) = \begin{cases} 0, & \text{if } r < d, \\ 1, & \text{if } r \geq d. \end{cases} \quad (1.69)$$

For dense packing, pairs of spheres are separated by $r = ah$, where a is any real number starting from 1. Then the PDF can be represented by a set of delta functions:

$$g(r) = \sum_i \delta(r - ia) \quad (1.70)$$

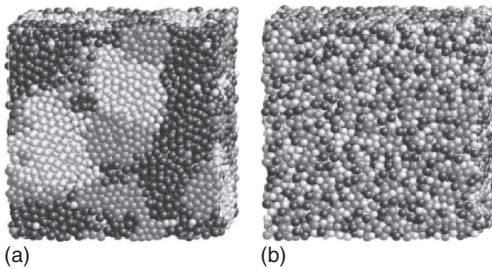


Figure 1.32 Probability of contacts on mixing spheres of different types. (a) Spheres separated into same type regions. (b) Spheres mixed at random.

The radial PDF is defined to be independent of orientation. In statistical mechanics, it is given by the expression:

$$g_{AB}(r) = \frac{1}{N_A N_B} \sum_{i=1}^{N_A} \sum_{j=1}^{N_B} \langle \delta(|\mathbf{r}_{ij}| - r) \rangle \quad (1.71)$$

1.4.8.2 The Probability of Contacts

Probability of contacts between atoms is frequently evaluated in condensed matter physics. For instance, to a first approximation the internal energy, U_{int} , of a thermodynamic system comprising two types of atoms is predicted to be:

$$U_{\text{int}} = N/2 [(c_A u_{AA} + c_B u_{BB}) - c_A c_B (u_{AA} + u_{BB} - 2u_{AB})] \quad (1.72)$$

where $c_A = N_A/N$ is the concentration of A-type atoms with specific interaction energy of u_{AA} , and c_B is the concentration of B-type atoms with specific interaction energy u_{BB} , respectively. The last term in Equation 1.72 expresses the enthalpy of mixing, which turns out to be a quadratic function of the probability of contacts between atoms A and B; this probability is expressed by the product of concentrations, $c_i c_j = c_A c_B$, and it is given by the statistical formula:

$$P_{ij} = \delta \cdot c_i \cdot c_j \quad (1.73)$$

where i and j stand for A and B, respectively, and δ has a value of 2 when $i = j$, and a value of 1 when $i \neq j$. The expression is verified for variety of sphere sizes, except for situations when one sphere is so small as to fit into an interstitial position between the large spheres.

1.4.8.3 Contact Configuration Function

Edwards and coworkers (2002) postulate a statistical mechanics approach to jammed (Torquato *et al.*, 2000) configurations. In particular, they develop the concept of entropy of micro-canonical ensemble of jammed configurations expressed as follows:

$$S = \log \int \delta(V - W(\varsigma)) \Theta(\varsigma) d\varsigma \quad (1.74)$$

where δ is the Heaviside function, V the volume of the body of N spheres (analogous to the internal energy of a system), ς the collective coordinates

of contact point positions in the static packing and $W(\zeta)$ a volume function expressed in terms of contact variables (analogous to the Hamiltonian of a system in statistical mechanics). According to Edwards, under the condition, $V = W$, the system is said to be ‘jammed’, and the function $\Theta(\zeta)$ ensures that all spheres are in fixed (locked) positions.

It is conjectured that it may not be possible to obtain an IAS (ideal amorphous solid) by any experimental method, just as it is impossible to grow an ideal, completely defect-free crystal. Certainly, all experimental attempts at random packings of spheres suffer at least three limitations that prevent even a close approximation to IAS. First, the force of gravity: its effect during the dynamic stage of pouring causes some clusters of spheres to arrange into locally close packed configurations (fcc and hcp) or to rearrange into these at a later stage by tapping or vibration. Second, friction: it limits the freedom to form random configurations and it is likely to be responsible for loose spheres in the structure. Third, inhomogeneity: this results from the directionality of pouring of the spheres into a container and also from edge effects because of the presence of the container walls. All three limitations can be avoided by computer simulation of round cells, as described herein.

1.5

Ideal Amorphous Solid (IAS)

We call a body consisting of randomly packed spheres *an* ideal amorphous solid (IAS) if it is constructed by following precisely the packing rules of Section 1.4 and therefore contains absolutely no imperfections of packing of any kind. The IAS is defined with the same purpose as one defines an *ideal crystal* in the theory of crystallography. The term *ideal* denotes perfection of structure, theoretical and hypothetical. It is meant to provide a universal model for representing and understanding the structure of amorphous solids, in a way analogous to crystallography, with the following advantages:

- 1) It uniquely defines the structure of the amorphous glassy solid by specifying the atomic arrangement, atomic radii, concentrations and chemical elements.
In particular:
 - a. all spheres are in fixed positions (i.e. perfect solidity), and the positions of the spheres are specified by the expression:
- $$S_{a,b,\dots,m} + X_{\text{IAS}} \quad (1.75)$$
- b. coordination distribution function, $\Psi(k)$
 - c. configuration distribution function, $\Phi_k(\zeta)$
 - d. free volume = 0
- 2) The IAS represents the base-line model for random atomic arrangement in amorphous solids and can be used to predict:
 - a. the *ideal* radial distribution function
 - b. the *ideal* coordination distribution

- c. the *ideal* configuration distribution
- d. the *ideal* structure factor
- e. the *ideal* X-ray scattering patterns
- f. the *ideal* physical properties
- g. and so on.

The centres of any three adjacent but non-touching spheres form triangles of unequal sides, due to (i) random positions and/or (ii) different sphere radii. There is not a single incidence of four adjacent spheres that are co-planar, in direct contrast to any of the crystallographic Bravais lattices where the multiple centres of spheres are co-planar. Consequently, there is no translational symmetry in this structure.

The condition of solidity and rigidity is implicit in the concept of an ideal amorphous solid, and the same is true for an ideal crystalline solid. The rigidity of every sphere is achieved with the conditions stipulated in Section 1.3. The geometrical construction of IAS lends itself readily to description and analysis by Voronoi tessellation and associated Delaunay simplexes.

The coordination numbers, based on touching neighbours, will be range bound to $k_{\min} \leq k \leq k_{\max}$, where $k_{\min} = 4$, and the value of k_{\max} will depend on the composition of the IAS and the specific cluster selected. In arrangements composed of different sized spheres, one can use the values for k_{\max} listed as a function of the ratio r_0/r_i , relying on calculations from Clare and Kepert (1986).

The statistical functions, $P_k(\zeta)$ and $\Psi(k)$ defined in Section 1.3, characterize the randomness of the packing arrangement. These functions provide a novel way to describe the structure of randomly packed spheres. Additional structural measures are described in Chapter 2, as well as by:

- X-ray scattering (described in the next chapter)
- Pair distribution function (described earlier in Section (2.1))

X-ray scattering is a direct corroboration for the conjecture that atomic arrangement in amorphous solids is random. The conjecture is based on the fact that the scattering property is a Huygens-style sum of amplitudes from all points of scattering and Fourier transforms. For instance, the local density at point, \mathbf{r} , is related to the average density multiplied by the radial distribution function, $\bar{\rho} \times g(r)$; the radial distribution function can be derived from the X-ray scattering measurements, and the scattered intensity is computed from the Debye equation. All of these relations are well established (Torquato, 2002).

That no short-range order (SRO) exists in the IAS random packing of spheres can be reasoned as follows. As all spheres are identical, variation in packing arrangement is the only source of differentiation. Then each cluster can be described by (at least) three statistics: (1) the number of contact points, k (2) the configuration of the nearest neighbours of the inner sphere, described by ζ , (3) the orientation of the cluster in space, described by some measure, Ω .

For two clusters (say, 1 and 2) to be identical, it is necessary that

$$k_1 = k_2, \quad \zeta_1 = \zeta_2, \quad \text{and} \quad \Omega_1 = \Omega_2.$$

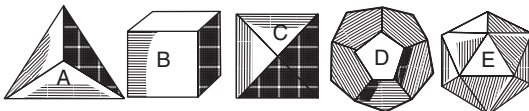


Figure 1.33 The five ideal Greek solids.

Each cluster has nine possible values for $k = 4, \dots, 12$. If the distribution for k is equiprobable, then the probability that two clusters have the same number of contact points (the same value of k) is simply $1/9$. For any given distribution $\Psi(k)$, as shown in Figure 1.16, we can write more generally that the probability for two clusters to have the same value of k is given by $\sum_{k=4}^{12} [\Psi_k]^2 = C/9$, where $1 < C < 9$ is some known constant if Ψ_k is known.

For the other two variables, we note that two independent copies of random variables with continuous distributions agree with probability 0. Therefore, the probability that two or more neighbouring clusters have identical coordination and configuration and are oriented in precisely the same way, is zero. Repeatability of an ordered or regular pattern in adjacent clusters extending along any line is zero. Consequently, it can be stated with generality that the IAS body has no short-, medium- or long-range translational and/or orientational order.

Such an ideal amorphous solid has no free volume, $v_f = 0$. From this condition, it can be deduced that such an ideal amorphous solid would possess Frenkel and Orowan theoretical strength and that its coefficient of diffusivity would be equal to zero, $D_{IAS} = 0$. These properties are also true of a perfect single crystal as defined by crystallography.

The IAS is an isotropic body when considered at a sufficiently large size. For real amorphous materials, this size is of the order of 10–100 nm (see the definition of representative volume element in Chapter 2).

The ancient Greek philosophers also identified and documented the so-called ideal solids, known as *Platonic solids*, shown in Figure 1.33. They are *regular polyhedra*, also called *ideal* because each, without exception, is made up of identical faces; the tetrahedron has four identical equal-sided triangles, the cube has six identical squares faces, and so on. In other words, a regular polyhedron has all faces as regular polygons, identical in both shape and size. These solids have resulted from a meticulous study of the properties of geometrical shapes. However, it may be imagined that these ideal shapes have also given ideas as to the appearance of mineral single crystals. In addition, they were used for the size of heavenly spheres of the universe (see books on Copernicus or Kepler).

1.6

Construction of an Ideal Amorphous Solid Class I

The construction of the IAS model is based on the hard sphere packing principles described in this chapter. It can be carried out using the IAS software,

which is available as freeware and can be downloaded from the web site: <http://users.cecs.anu.edu.au/~u9300839/index.php>

The IAS software is written in MatLab, and it remains the copyright of the authors as indicated in the User Instructions included with a complete download. The download software includes all the packages necessary to run the software. The first part of the program creates a virtual round cell of randomly packed spheres according to the IAS rules described in this book. The second part analyses the packing and provides results for

- packing fraction
- Voronoi packing fraction
- pair contact probability
- radial distribution (PDF) by centre statistics
- radial distribution (PDF) by centre statistics (fine graded)
- coordination distribution statistics by contact and by Voronoi method
- random walk vector magnitude
- Voronoi volume statistics
- equally divided points on central sphere
- IAS visualization
- X-ray scattering

The starting point of construction of an IAS model is the creation of an irregular primary cluster, as shown in Figure 1.35, by any of the two methods described in this chapter. This function is in-built into the IAS software. Entering a call for the IAS-GUI opens up the following dialog as shown in Figure 1.34.

To enter data in IAS graphical user interface (GUI) click in the field [At. symbol], then a new window with a table of chemical elements will open. In the table of

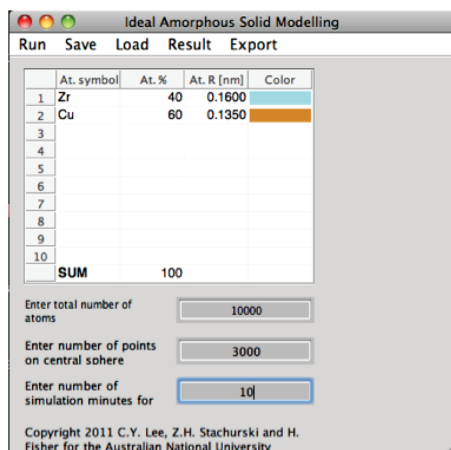


Figure 1.34 (a) The IAS-GUI dialog at the start of the program.

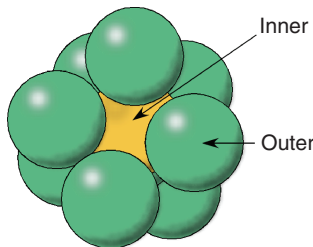


Figure 1.35 Distinction between inner and outer spheres in a primary cluster.

elements, click on the desired element. The element symbol, its atomic radius, and its colour will appear automatically in the IAS-GUI.

Repeat the above-mentioned actions for additional elements, as required.

Finally, assign atomic percentage(s), in the field(s) – [At. %], for each element such that the SUM of [At. %] adds up to 100.

Note: The radius of each element can be changed by clicking on the corresponding field and entering the data manually. The colour of each element can be changed by clicking on the corresponding field and selecting it from the colour chart.

In computational terms, division of the sphere's surface into equally spaced points results in a list, which may be denoted as $\mathbf{L}[\mathbf{x}_n, p]$, where p are the point sequential numbers and \mathbf{x}_n the points' corresponding coordinates, x_p, y_p, z_p . For all $1 \leq p \leq n$, $x_p^2 + y_p^2 + z_p^2 = R^2$, where R is the radius of the inner sphere. The number of chosen points depends on the required outcome. The larger the number, the greater the division and the finer the random positioning of the outer spheres. The smaller the number, the lower the memory requirements and faster execution of the program. It has been found by experience that $n = 3000$ points is a minimum workable number for this purpose.

Once the list has been compiled, the program chooses at random a point from the list. A random number, \mathcal{R} , is generated in the range $0 \leq \mathcal{R} \leq 1$, which is multiplied by n , so that a point, $p = \text{Integer}[n \cdot \mathcal{R}]$, on the list is chosen. As k points will be finally selected, the first can have id number, $k = 1$, assigned to it.

For each subsequent point ($k > 1$), a check must be made to ensure no overlap of spheres, see Figure 1.36. The geometric condition is for an angular separation to avoid overlap onto each other's excluded space. This condition is correct for the case of monoatomic size, that is $|\mathbf{R}_\ell| = |\mathbf{R}_k|$ for all $1 \leq \ell \leq k$. If the condition is satisfied, then the $k = \ell$ point is selected and its coordinates stored in memory. This loop process is continued until no further points can be added to the inner sphere. The end result is a list of k points with their respective coordinates, all satisfying the non-overlap condition.

For the case of spheres of different radii, the lower limit, $\pi/3$, will be smaller or larger, depending on the actual sphere sizes involved, which is resolved geometrically.

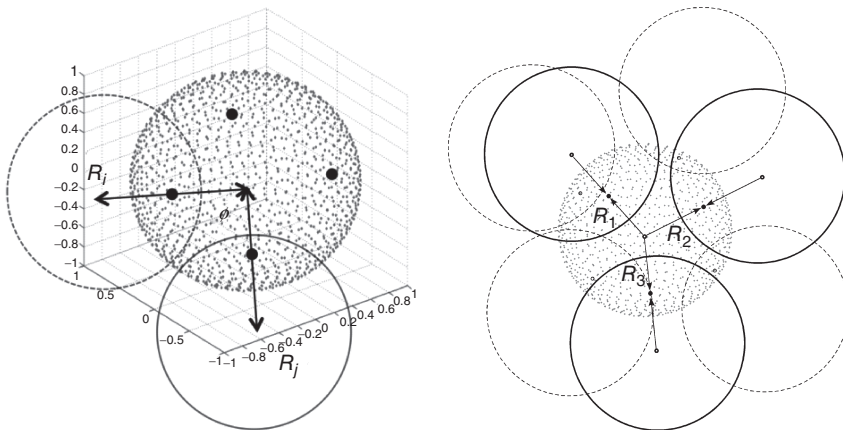


Figure 1.36 Selected points are tested for overlap.

The end of this process is reached when the blocking function, $\hat{b} = 1$. This means that none of the remaining free space around the inner sphere is of sufficiently large extent to allow the addition of another sphere onto it. In principle, this is a straightforward and easily understood condition. In practice, it is not so simple because there is no analytical function describing the blocking function, so it cannot be coded analytically. Instead, an algorithm is made to delete p -points from the original **L**-list until none are left; then the program is halted. The deletion of the p -points occurs for every successful and every unsuccessful point selection. In the former case, all points lying within the spherical cap around the selected point and extending over the conical angle, $\phi = 2\pi/3$ are deleted. In the latter case, only the selected point is deleted. As n is finite, the execution of the program is finite and relatively quick.

To complete the construction of the primary cluster, a sphere is placed in contact with the inner sphere at the chosen k points. Consequently, the distance between centres of the inner and outer spheres is $2R$ for a monoatomic model or $R_m + R_{m+1}$ for a model involving m atomic sizes.

With the primary cluster completed, the following important observations can be made.

- The centres of any two outer spheres of the same size make an isosceles triangle with the centre of the inner sphere.
- For a multi-size case, the maximum number of spheres that can be made to touch the inner sphere depends on the specific case. However, it can be stated categorically that \hat{k} for that model is always less than k_{\max} .
- For any three adjacent outer spheres in a given shell, the distances between their centres are unequal. This means that the centres of any three adjacent spheres form *irregular triangles*. Consequently, the seed cluster is an irregular cluster (Figure 1.37). This is a fundamental requirement for the construction of an ideal amorphous solid model.

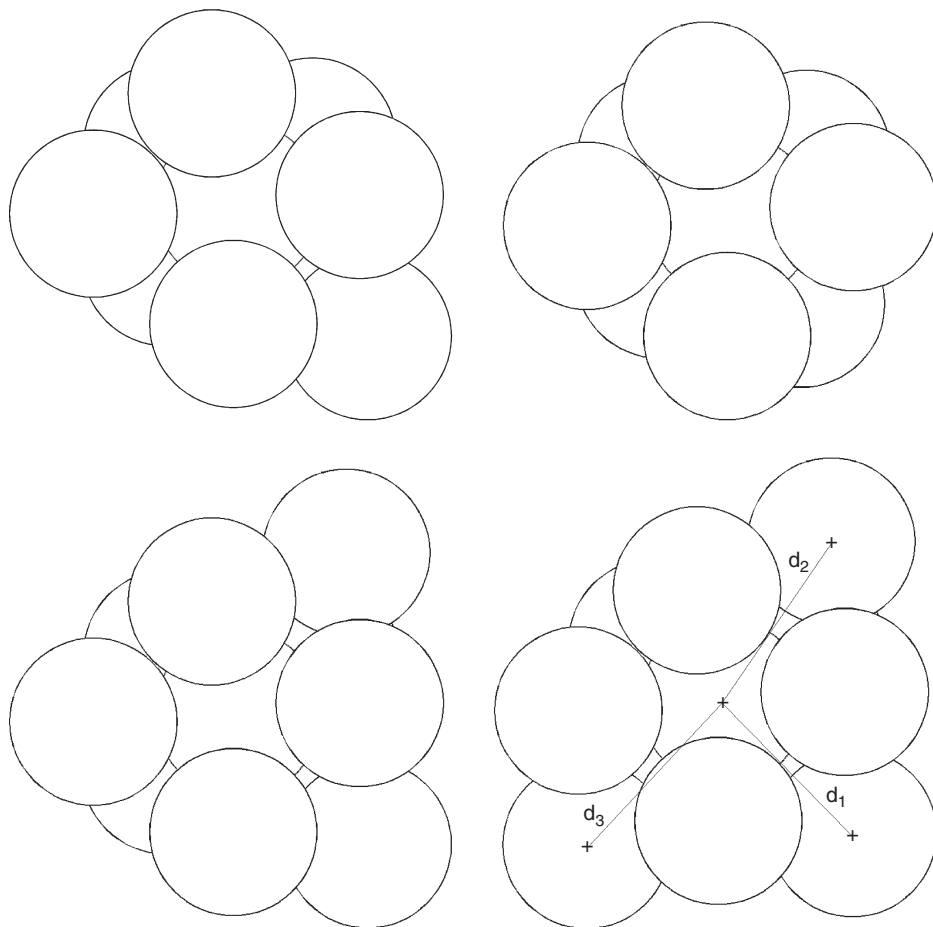


Figure 1.37 Second layer growth of an irregular primary cluster with initial $k = 8$. Three additions are shown with $d_1 \neq d_2 \neq d_3$.

Growth of the primary cluster is achieved by addition of spheres to three-sphere sites. As shown in Figure 1.37, an irregular primary cluster with $k = 8$ has the first sphere in second shell added onto three-sphere site with the closest distance to the inner sphere; then a second sphere is added onto a three-adjacent-spheres site; then a third sphere is added ($d_1 < d_2 < d_3$), and so on, until the shell is filled in.

In the appropriate field of the GUI, enter the total number of atoms (to be simulated): any number between 1 and 10^6 is acceptable. Figure 1.38 (below) shows a previously simulated round cell comprising 10^6 atoms in a metallic glass composed of 65% Mg, 25% Cu and 10% Gd atoms.

Next, enter the number of points on the central sphere: typically 3000, as shown in Figure 1.39. This is the number of computed equidistant points on the surface of the first inner sphere. The outer spheres will be added by the program onto

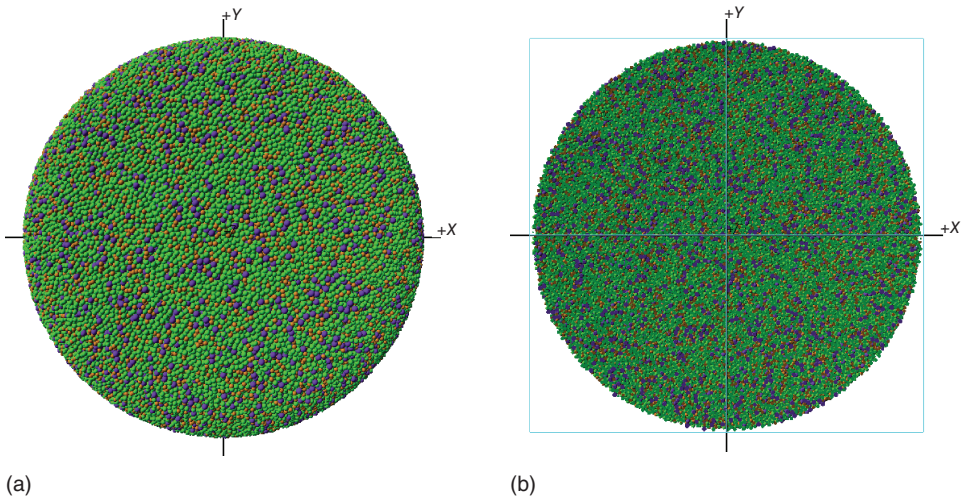
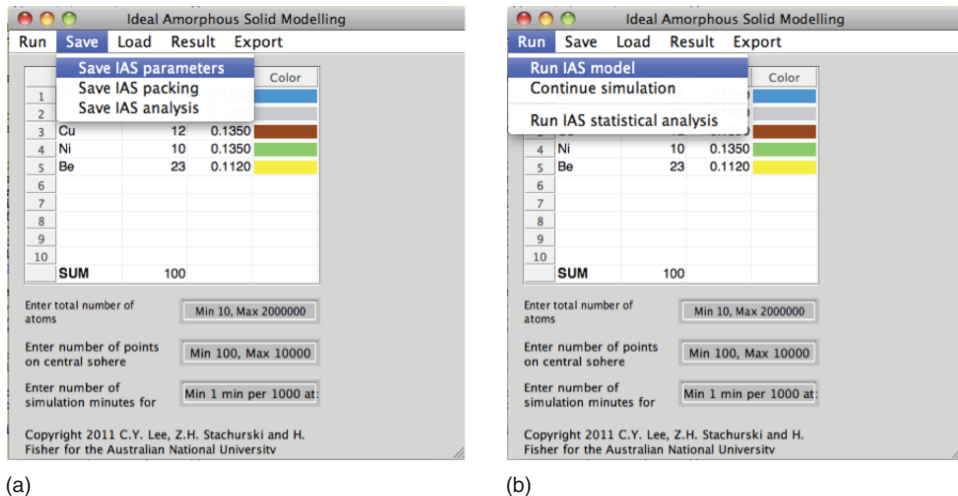


Figure 1.38 (a and b) A view of a round cell and its cross section, comprising 10^6 spheres of three different sizes.



(a)

(b)

Figure 1.39 (a and b) Two views of the IAS main dialog.

points randomly chosen on the surface of the central sphere as described earlier. Consequently, the outer spheres will form an irregular cluster. The program will accept any number between 1 and 10^5 .

Enter the number of simulation minutes. Suggested numbers are 2 for 10^4 spheres, 20 for 10^5 spheres and 200 for 10^6 spheres.

Finally, save the IAS parameters (Figure 1.39). The software directs the file to the 'IAS parameters directory', to be found in the IAS software folder. The outcome of this process is a three-dimensional geometrical pattern of randomly packed



Figure 1.40 A wait bar will open during simulation.

spheres, called a *round cell* if it is of finite dimensions or an IAS if it is of infinite extent. The essential information about the round cell is stored in a matrix, $\mathbf{M}[\mathbf{x}_N, m]$, where N is the total number of atoms/spheres in the model, the vectors \mathbf{x}_N define the positions of the sphere's centres with respect to the origin and m identifies the corresponding type of the sphere, usually by its radius. Example of a round cell and its cross section is shown in Figure 1.38.

Go to the RUN menu and select 'Run IAS model' as shown in Figure 1.39. A wait bar will open and indicate progress of the simulation (Figure 1.40).

1.7

Elementary Theory of Amorphousness

1.7.1

Background

A theory is a collection of logically interrelated ideas on and descriptions of a particular topic. The ideas may include axiomatic statements and subsequent deductions that form a self-consistent framework of knowledge on a given subject. Therefore, a theory involves logical analysis and reasoning from assumed premises; it puts forward a hypothesis to be maintained or disproved. Furthermore, a theory is used to explain data and generate hypotheses that can be tested by research.

A personal knowledge is an *understanding* of the studied topic. It involves *experience* (skills and familiarity) and requires *holding in memory*:

- 1) an amount of information (i.e. a number of facts)
- 2) a concept of relationship(s) between the elements (parts) of the information
- 3) an ability to manipulate the concepts and facts to derive and present reasonable and logical arguments

The level (depth) of understanding, and therefore the level of knowledge, depends on the amounts of (1) and (2) and the ability in (3).

An overview of the field of solid state, and of its corresponding theories, can be summarized as shown in the table below. There are three main divisions of the solid state: crystalline, quasi-crystalline and amorphous. Each area has a corresponding geometrical theory that defines the ideal solids in terms of perfect packing of spheres or (for the case of quasi-crystalline state) other geometrical objects.

Solid-state fields		
Crystalline	Quasi-crystalline	Amorphous
Theory of crystallography Ideal crystalline solids	Theory of quasi-crystallography Penrose tiles	Theory of amorphousness Ideal amorphous solids

This representation can be followed by associated theories of solids containing imperfections.

Solid state fields		
Crystalline	Quasi-crystalline	Amorphous
Theory of crystal defects	Theory of imperfections	Theory of imperfections

Certainly, theory of crystal defects and theory of crystallography are well developed. Presently, this cannot be said of the other two fields.

There are several methods to test a theory. However, the foremost kind of testing is to verify the predictions of the new theory. If it is verified, then the theory has, for the time being, passed the test; there are no reasons to discard it. The amount of empirical information conveyed by a theory, or its empirical content, increases with its degree of falsifiability. A theory is falsifiable if there exists at least one class of non-empty basic statements which are forbidden by it. According to Karl Popper, the larger that content of the class the more falsifiable is the theory. It also means that the theory says more about the world of experience than a theory with fewer falsifiable statements.

A special random packing that corresponds to the packing in ideal amorphous solid is characterized by properties of and limitations imposed on the set X_{IAS} , summarized from Section 1.4, and shown below:

1.7.2

The Axioms

- A1. Choose any two spheres in the IAS packing and draw a straight line passing through the centres of the two spheres.

Then, the probability of any other sphere in the packing having its centre lying on that line is zero.

- A2. A straight line of arbitrary direction passing through an IAS will be divided by the atoms/spheres that it cuts through (or is tangent to) into irregular

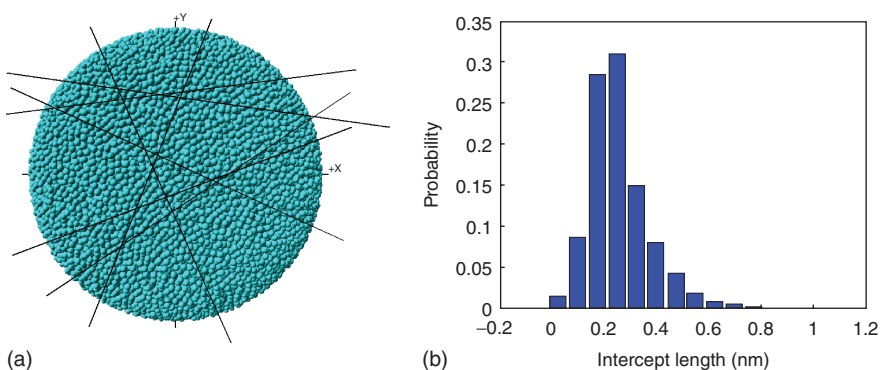


Figure 1.41 Illustration of the axioms A1 and A2: (a) straight lines cutting through the IAS model at random orientations and (b) distribution of irregular line segments in a monoatomic IAS. The graph is a summary statistics of segments from 10^3 lines.

length segments, in contrast to crystalline solids where interatomic distances are always regular (providing the line has a rational slope).

- A3. For any IAS, the statistical distribution of lengths of the irregular line segments will be the same regardless of the direction of the line as a consequence of the solid being homogeneous and isotropic.

Figure 1.41 is an illustration of the concept expressed by the last two axioms earlier. The round cell, shown on the left, contains 10^6 sphere of the same size, and the graph on the right contains the corresponding statistical data.

1.7.3

Conjecture

It is conjectured that there exists an ideal random packing of spheres, constructed in accordance with the above-mentioned rules and possessing the properties and complying with the limitations given in Tables 1.7 and 1.8. Then,

$$X_{\text{IAS}} = X_{\text{RCP}} \quad (1.76)$$

Table 1.7 Global properties of the set X .

	Property	Object	Requirement
P1	scale invariance	if $S_a + X$ is a packing	$S_{ca} + cX$ is also a packing
P2	homogeneity	let $N = [xn]$ be a point field and $N = [xn + x]$ is a point field	both fields must have the same distribution for all $x \in E_n$
P3	isotropy	if $N = [xn]$, and $R(\theta)N = R(\theta)[xn]$	have the same distributions then the field is isotropic

Table 1.8 Limitations imposed on the set X .

	Limitation	Object	Requirement
L1	solidity	all spheres in <i>fixed</i> positions	touching hard spheres
L2	coordination, k	for any point $x_\ell \in X$	$ x_{\ell j} - x_\ell = a$ $4 \leq k \leq 12$ with probability $\Psi(k)$
L3	configuration, ζ	for any cluster centred on $x_\ell \in X$	$0 \leq \zeta \leq \zeta_{\max}$ $\Phi_k(\zeta)$

Such an ideal random packing of spheres is a model of atomic arrangements in an ideal amorphous solid, as described in this book.

1.7.4

The Rules

Structures of any kind are purposefully created by following carefully designed rules of construction. The rules for creating a model of an ideal (theoretical) amorphous solid should be considered as analogous to the rules for creating a perfect (ideal) crystalline arrangement. However, the resultant amorphous structure must contain none of the elements of symmetry present in crystalline arrangements, such as mirror, rotation or glide. Therefore, to create an amorphous packing of spheres, the rules must not enforce any ordering beyond the nearest neighbour and therefore can apply only to adjacent spheres. Such basic rules for amorphous packing of spheres can be expressed as follows:

- R1. Every sphere must be in *fixed* position so that the resultant structure is solid.
A sphere is in fixed position when for $4 \leq k \leq 9$ touching contacts with neighbouring spheres, no more than $(k - 1)$ are located on one hemisphere; for $k > 9$, a sphere is always in a fixed position.
- R2. Three adjacent non-touching spheres must form an *irregular* triangle, so that no two triangles have the same (identical) shape.

The first rule requires that all spheres in the amorphous packing must have touching contacts and that the number of contacts for any individual sphere in a monoatomic structure is limited to the range of $4 \leq k \leq 12$. This packing of spheres models a perfectly rigid solid as no sphere in the body can be moved in any direction.

The second rule implies that in each cluster there are adjacent but non-touching spheres, with distributed distances between them limited to the range: $2r < D_{ij} << 2\sqrt{3} r$. A consequence of this packing arrangement is that no four adjacent spheres (touching or not) lie in a plane. It ensures that none of the symmetry elements, characteristic of crystalline arrangements, are present in the amorphous body.

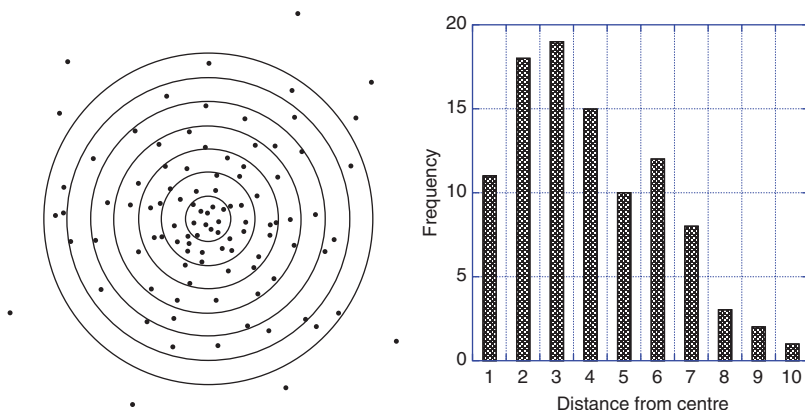


Figure 1.42 Target with randomly distributed shots and a corresponding Gaussian plot.

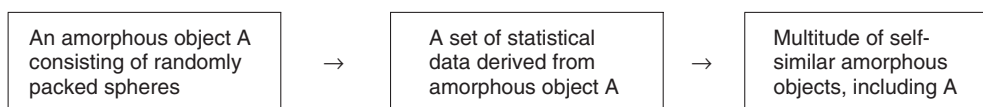
It transpires that, under the above rules, there are no solutions for random packing of spheres in one or two dimensions. In three dimensions, the IAS proposed by To *et al.* (2006) is a solution for a perfect random packing of spheres obeying the rules and axioms listed earlier.

A final point to be made here is that an ideal amorphous structure is not the same and not equal to a thermodynamic ideal structure. The former is purely a geometrical construct, the latter is particular state of physical matter.

1.7.5

Statistical Correspondence

A geometrical theory of amorphousness can be postulated on the basis of statistical correspondence, two related axioms and two rules, as described in the following. The condition of correspondence in statistical geometry limits the reconstruction of events from their descriptive distributions. For example, given a distribution of shots fired at a target, one can confirm by analysis that it is Gaussian (Figure 1.42), but from the given distribution, it is not possible to reconstruct the precise positions of the shots. A schematic representation of this relationship is shown in the diagram below:



This is in contradistinction to an ordered structure, which can always be reconstructed identically from its unit cell and symmetry elements.

Analysis of the packing of spheres, $S + X$, gives information that is uniquely derived from the packing. However, the reverse relationship is not unique; from the given information for a random packing, one can recreate not one but a

multitude of packings (multitude of sets X) of the same characteristics and properties, including the one identical to the original.

1.8

Classes of Ideal Amorphous Solids

At this stage of theoretical development, three separate classes of IAS can be distinguished:

- IAS Class I—represented by random packing of spheres as described in the previous section.
- IAS Class II—represented by random packing of spheres with local SRO.
- IAS Class III—represented by random three-dimensional networks without any local order.

1.8.1

IAS Class I: Random Close Packing of Individual Atoms

The random packing of hard spheres in fixed configurations, as described in the previous sections, represents packing of individual atoms with no preference for, and no bonding to, nearest neighbours. It is proposed that IAS Class I is a good model suited particularly to metallic glasses. It is the most general, least restricted IAS model from which other classes can be derived. Its only correlations are limited to the touching neighbours. Otherwise, this class has no short-range, no medium-range and long-range correlations present.

1.8.2

IAS Class II: Random Close Packing of Linear Model Chains

The IAS Class II has similar characteristics of the IAS Class I, with the addition of SRO between specific nearest neighbours that are bonded. This means that the bonded neighbours do not separate when flowing or in the liquid state and therefore represent linear, chain-like random atomic arrangements found in organic and inorganic glasses.

Consider a simulation cell containing N randomly close packed equal-sized touching spheres, that is IAS Class I (where N is a large number). Convert it to Class II by making a chain of touching spheres by the following process: Choose one sphere as the starting point and link it with one of its touching neighbours. Next, link the second sphere at random with one of its touching neighbour, except the one already joined to. Continue in this manner the three-dimensional SARW, linking spheres until a chain of $(n - 1)$ links is made.

Next, chose another unattached starting sphere, and following the above-mentioned process construct another chain of n spheres. Repeat the process until (N/n) chains are formed. As $N \gg n$, there are many ways to form the

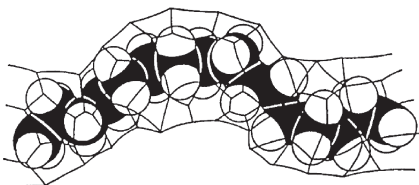


Figure 1.43 Representation of a segment of polyethylene macromolecular chain with C and H atoms to scale and a schematic drawing of Voronoi tessellations.

chains, and therefore, there exists a finite probability that it is possible to form (N/n) chains without violating the SARW or creating cross-links, and without any 'free' sphere(s) left over. This cell of linear model chains (macromolecules) constitutes an ideal polymeric amorphous solid of Class II. Such a simplification of the molecular chains has been used in the science of polymers which can be found in relevant textbooks. This approach has been used for the results shown in Figure 1.25. If the monomers in the chains are represented by spheres, then IAS Class II is indistinguishable from IAS Class I.

However, more accurate representation of macromolecular chains requires modelling of atoms to scale, for example as shown in Figure 1.43 for polyethylene. The H atoms are drawn in towards the C-atom in each monomer due to strong covalent bonding, and therefore representing CH_2 group as one sphere is possible, but usually quite inaccurate.

The degrees of freedom of a chain in IAS-II are defined by free rotation around each link and are constrained by (i) the fixed distance between linked spheres and (ii) the angle between neighbouring links being limited to $60^\circ \leq \Theta \leq 180^\circ$. Therefore, rotations and translations are coupled. In a chain segment in which the first and the last spheres are in fixed positions, we find that

- 1) in a segment containing three or four spheres, all are in fixed positions imposed by their bonds, regardless of other contact points,
- 2) in segments longer than four spheres, the middle spheres acquire loose position properties, unless fixed by contacts with other surrounding spheres,
- 3) for chains with fixed valency angle (typically $\Theta = 109^\circ$), sufficient kinematic freedom appears in segments of seven or more links.

The kinematics of chains is a subject of its own in the field of mechanics. The analysis of linkages requires co-ordinate transformations around a closed chain which must satisfy the following relationship for each and every configuration:

$$[T_{n,1}] \dots [T_{34}][T_{23}][T_{12}] = [1] \quad (1.77)$$

where [1] is identity matrix and $[T_{i,j+1}]$ transforms coordinates of a point P in i system to its coordinates in $i + 1$ system. Suffice it to say that analysis of a model chain based on polyethylene with seven links can be shown to satisfy the condition for general deformation, providing the end of the chain P is confined to move in limited space.

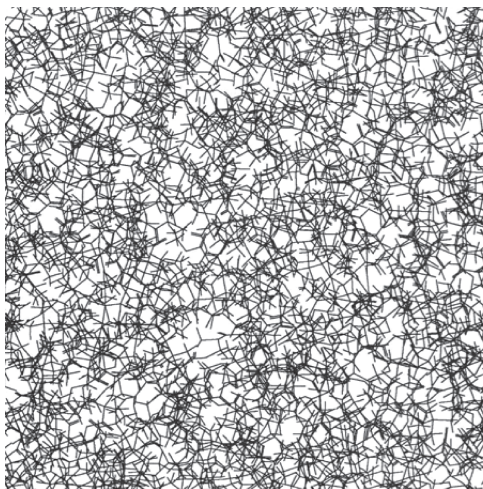


Figure 1.44 Randomness of bonds in a computer-simulated cell of cross-linked polymer.

1.8.3

IAS Class III: Random Close Packing of Three-Dimensionally cross-Linked Chains

Presently, there are no models of ideal packing of chains of this kind based on packing of spheres. The structure of cross-linked polymers is described by other methods; one way of representation of the randomness of the structure is by displaying the skeleton of bonds only, omitting the atoms, as shown in Figure 1.44.

1.9

Imperfections in IAS

Perfection of structure is defined firstly by the definition of imperfections that may occur, and secondly by the strict requirement of the absence of those imperfections, namely no blemishes, flaws or defects of any kind, for which we shall use the collective term *flaws* (in contrast to ‘defects’ used in crystalline solids). For example, a gas in which the particle velocities conform precisely to the Maxwell distribution is referred to as an *ideal gas*; any deviation from this distribution is an imperfection and its behaviour will deviate from that of the ideal gas law. In the same sense, in an ideal amorphous solid, the arrangement of spheres conform precisely to distributions consistent with the functions $\Psi(\kappa(x_\ell))$ and $\Phi_k(\zeta)$; any deviation is then an ‘imperfection’. Two general categories of flaws in the random amorphous structure can be defined: (i) geometrical and (ii) statistical, as described in the following.

The classical science of crystallography describes ideal crystalline solids by emphasizing their perfection, which is defined (by common usage) as the physical

state of total absence of imperfections. Then, defects in crystalline solids are defined with regard to the perfection of the ideal crystalline structures. Defects introduce disorder in ideal crystalline solids and alter their behaviour. Many properties of real crystalline solids (both natural and synthetic materials) are governed directly by the presence of defects in their structure. For example,

- *Diffusion is governed by the density of vacancies or interstitials (point defects)* (Flynn, 1972)
- *Screw dislocations in zeolites can confine diffusion to one direction only (line defects)* (Walker et al., 2004).
- *Plastic deformation is understood mainly in terms of dislocation glide (line defects)* (Cottrell, 1965) or grain boundary sliding (surface defects) 1975.
- *Semiconductors are created by doping crystals (introducing defects) to modify their electronic structure (point defects)* (Turek, 1997).

The significance of these relationships is reinforced when realizing that no diffusion is possible without defects that crystals reach their theoretical strength if no dislocations are present and that semiconductors become insulators if doping is removed.

1.9.1

Geometrical (local) Flaws

We distinguish three kinds of geometrical flaws that can occur in the IAS-I structure:

- 1) spheres of different sizes (as impurities)
- 2) loose spheres
- 3) vacancies/holes
- 4) compositional inhomogeneities.

In an ideal amorphous solid composed of spheres of the same size, any sphere of a different size must be considered as a geometrical (and structural) flaw, as would be the case in ideal crystalline solids (substitutional or interstitial defect). On a local level, such a different sphere may have its contact number outside the allowable range, depending on the size difference. On a larger scale, the effect of its presence would be evident (if in sufficient concentration) in the radial distribution function or equivalently in the structure factor. Loose spheres possess limited freedom of movement within the cage created by its neighbours. A quantitative measure of the movement of any sphere (labelled, say i) is given by the value of the displacement (Equation 2.43), where u_i , v_i and w_i are components of the allowable movement (in a Cartesian frame of reference) relative to its neighbours. By definition, for a fixed sphere, $J_\ell = |\mathbf{J}_\ell| \equiv 0$; for a loose sphere, $0 < J_\ell < a$ because here we do not allow a vacancy. The definition of IAS requires that $\mathbf{J}_\ell \equiv 0$ for $i = 1, \dots, N$, that is all spheres are in fixed positions.

A *vacancy* is defined as an empty hole (unoccupied space) with its minimum dimension equal to or greater than the diameter of a sphere ($l_{\min} \geq a$). It is considered as a serious flaw having a significant effect on the overall density of IAS. The condition that all spheres are fixed is sufficient to disallow the occurrence of vacancies in the IAS-I. An exception is the special case of clusters of 13 touching spheres with either fcc ($k = 4 + 4 + 4$) or hcp ($k = 3 + 6 + 3$) packing arrangement. In these cases, removal of the central sphere would result in a vacancy with the surrounding spheres remaining in fixed (jammed) positions (Torquato *et al.*, 2000). The occurrence of such clusters is considered to be a statistical flaw in the IAS structure, as described later.

The existence of vacancies in crystalline solids is well proved; the existence of vacancies in real amorphous solids is a matter for debate. It is conjectured that in amorphous solids vacancies occur in the form of free volume distributed throughout the volume rather than concentrated at some specific points as vacancies. This proposition has support from the arguments presented in Section (1.4.5). In the IAS model for packing of spheres, individual clusters vary in their coordination number and packing fraction (or density) even though the free volume = 0. In real solids, interatomic forces are active and such density variations result in stored elastic strain energy, which will provide the thermodynamic driving force for (i) a certain degree of relaxation of density variations and (ii) free volume to become > 0 . The supposition is that free volume is trapped whilst cooling from the liquid phase. It is well known that densification of glasses can be achieved by annealing close to the glass transition.

1.9.2

Statistical (global) Flaws

It is possible to specify statistical flaws under two categories:

- 1) flaws associated with the $\Psi(k)$ function; and
- 2) flaws associated with the $P_k(\zeta)$ function.

With regard to the first category, a sphere with a contact number $k < 4$ constitutes a flaw in the ideal amorphous structure. It is both a statistical flaw with respect to the $\Psi(k(x_\ell))$ function in that it violates the allowable range of values in the variable and also a geometrical flaw in that it violates the requirement that all spheres be fixed. At the other end of the spectrum, we note that in Euclidean space no sphere can have $k > 12$. Such flaws cannot occur in any packing of spheres of identical diameter (physical impossibility). An important, and more likely, source of statistical flaws, is the departure from the *ideal* distribution of contacts predicted by the $\Psi(k(x_\ell))$ function. In a special packing, when the distribution becomes single valued (e.g. $k = k_{bcc} = 8$ for all atoms, and the half peak width, $\omega_\Psi = 0$), the body will acquire regular structure, which may be perfectly ordered, or disordered, but it is no longer amorphous.

With regard to the second category, any arrangement of contact points on a sphere which corresponds to any of the five regular arrangements (Greek solids)

is classified as a flaw because it represents an ordered (crystalline) structure and a departure from the prescribed distribution of contact points. More generally, any arrangement of contact points on a sphere which corresponds to equidistant angular configurations of points or any of the Bravais lattices is classified as a flaw. Specifically, clusters of 13 spheres with hcp or fcc arrangement are considered as serious flaws in IAS-I, in that these increase drastically the average density of the body. It should be noted that an icosahedral arrangement of 13 spheres ($k = 1 + 5 + 5 + 1$) is not a flaw because in this case the touching neighbours can be moved around the inner sphere (whilst remaining in contact with it). Hence, $0 \leq \zeta \leq d$ (where d is a constant), and the width of the distribution, $w_p > 0$. Furthermore, removal of the inner sphere from an icosahedral cluster of 13 touching spheres (symmetrical or not) will make the outer spheres loose. Therefore, it is neither a special case nor a statistical flaw.

1.9.3

The Effect of Flaws on the Density of IAS

The transition from liquid- to solid-like behaviour of randomly packed spheres is considered to occur at a packing fraction close to 0.49 (Reiss and Hammerich, 1986; Kopsias, 1998). This represents the lower limit for “solid” random packing of spheres. At the other end of the spectrum, the hcp or fcc arrangement of spheres represents the upper bound for sphere packing fraction at 0.74. Therefore, the atomic packing fraction p_{IAS} for IAS must lie within the range $0.49 < p_{IAS} < 0.74$. The packing density of the IAS model is in the range 0.63 ± 0.05 . There is no precise and unique value for the packing fraction as it depends on the composition, range of atomic radii, the coordination and configuration of the starting cluster and possibly other factors.

In a given experimental random packing of spheres (non-IAS), there must be flaws of the type described earlier. This view is supported by the results for simulated cells in which an increasing number of vacancies and loose spheres was shown to lower overall density. On the other hand, higher density random packing models, approaching a packing fraction of 0.64, show distinct splitting of the second peak in the radial distribution function, a clear indication of the presence of fcc or bcc clusters or their fragments or alternatively a spiral connection of tetrahedra or local icosahedral packing.

Flaws vitiate the structure of the ideal amorphous solid, causing its density to vary from the hypothetical ideal value. Loose spheres and vacancies have the effect of lowering the density, whereas an undue presence of fcc and hcp clusters tends to increase density, both locally and globally. Data from two separate studies in which the properties of simulated cells comprising large numbers of randomly packed spheres were described are sketched in Figure 1.45. First, round cells comprising randomly packed spheres around a central nucleus were created by computer simulation. An algorithm was devised to add spheres to an existing surface, starting at the nucleus. Round cells of different densities were obtained in one of two ways: (i) specific parameters in the algorithm were adjusted to reduce optimum packing

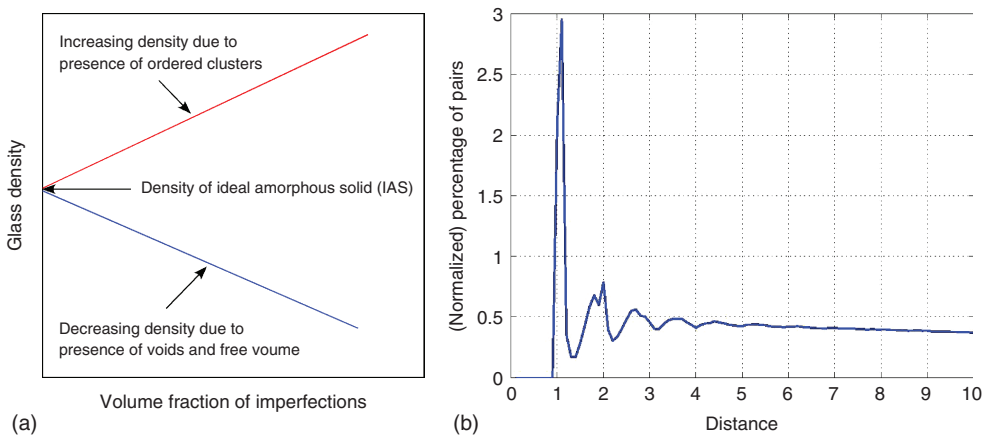


Figure 1.45 (a) The effect of packing imperfections on the density of IAS. (b) PDF showing split second peak due to packing imperfections (order).

and (ii) spheres were removed at random from a given cell of maximum density. As expected, global packing density decreases as the fraction of loose spheres increases. A line fitted to the data points, starting at 0.49 and 80% loose sphere content (solid-liquid transition point), and extrapolated to zero content of loose spheres, points to a value close to 0.63 ± 0.05 for the density of a packing containing none of these flaws. It is proposed that the round cell with the maximum packing density is a close approximation of IAS-I and that the most likely packing density of IAS-I is close to that value, measurably lower than the so-called typical value of 0.64.

In another publication, the so-called cylindrical cells were constructed by pouring a large number of hard spheres into a container whilst holding a stick in the middle of it; the stick was then removed, leaving a packing density of approximately 0.58. Higher densities, up to approximately 0.64, were achieved by gently tapping the sample. The packings were analysed by X-ray tomography and computational rendering of the spheres, so that geometrical properties of the packings could be measured. In particular, the results showed significant fractions of fcc and hcp clusters occurring in the samples. The data in Table 2 from Aste *et al.*, (2004) are also plotted in Figure 1.45, illustrating the relationship between the packing density and the combined fractions of fcc and hcp clusters. In this case, the global packing density of samples increases with the number of high density clusters which are considered as both geometrical and statistical flaws in the IAS-I. This is a remarkable observation in that we are accustomed to thinking of defects as always decreasing the density of crystalline materials, whereas a flaw in an ideal amorphous solid evidently can have either positive or negative effect on density, depending on the nature of the flaw. It is supposed that the two red square points at 5% flaw content, but well below 0.6 packing fraction, must correspond to cylindrical cells that retained the large number of loose spheres and vacancies expected from the method of construction, with a small content of fcc and hcp

clusters formed by gentle tapping. It is assumed that in these cells the presence of loose spheres and vacancies is the dominant flaw type causing overall reduction in packing density.

Now, consider the effect of short- and long-range ‘order’ as factors in density variations. By definition, SRO in solids refers to ordered packing of atoms in small volumes, ranging over one or two atomic distances. Ordered packing in a region (say, convex) means that one or more symmetry elements should be found in the arrangement of atoms confined to within that region. For any random cluster to exhibit SRO in itself, it would have to possess a minimum of one statistical geometry element. Examples of SRO in real materials include

- *Guinier-Preston (GP) zones in Al–Cu alloys*
- *cationic short-range order in crystalline ionic conductor*
- *i-phase nano-crystals in Zr-based bulk metallic glass (BMG)*.

The GP zones form in the shape of a disk with translational symmetry of AlCu_2 atomic groups along its basal plane and rotational symmetry perpendicular to its base. The second example refers to supercell structure within a Hollandite crystal consisting of TiO_6 and MgO_6 octahedra within a tetragonal unit cell. The third example represents near spherical particles with icosahedral configuration (quasicrystalline) appearing in the five element metallic alloy with random amorphous atomic packing. Is short-range ‘order’ possible in the random packing of spheres, and specifically, in an ideal amorphous solid Class I. We can disqualify compositional variation as all spheres are identical, leaving variation in packing arrangement as the only source of differentiation. Each cluster can be described by (at least) three statistics:

- the number of contact points k ;
- the configuration of the nearest neighbours of the inner sphere, described by ζ ; and
- the orientation of the cluster in space, described by the measure Ω .

We propose that if a monoatomic amorphous solid is an IAS then its structure must conform without exception to two statistical properties, subject to invariance under rotation:

- $\Phi_k(v_1, \dots, v_k), k = 4, \dots, 12$, is a family of joint probability density functions, on k unit vectors v_1, \dots, v_k in \mathbb{R}^3 , of the configurations of clusters of spheres.
- $\Psi(\kappa(x_\ell)), k = 4, \dots, 12$, a probability distribution for the number of nearest neighbours (coordination number).
- In geometrical terms, amorphous solids are fundamentally different from crystalline solids in that they cannot be constructed by the crystallographic method of translation of the basis along the lattice points. They do not possess any regular lattice.
- A random structure is not merely a disordered structure. A disordered crystal structure can be gradually restored to its fully ordered state by removal of its defects. In principle, an amorphous structure with flaws can be rearranged to its ideal (perfectly random) state.

- The IAS-I is an irregular assemblage of spheres containing no imperfections. By definition, it shows the absence of preferred local configurations and local flaws. It is of infinite extent (no edge effects) and shows no orientation. It is homogeneously random (it is ergodic with respect to detail of local patterns).
- Flaws in amorphous solids can increase or decrease average body density, depending on the type of flaw.
- The mean coordination number of spheres is rational in an ideal crystalline structure and hypothesized to be irrational in an ideal amorphous solid.

1.9.4

Short and Medium Range Order

We have concluded in Section 1.5 that the IAS packing has no short-range, medium-range, nor long range order. However, all real amorphous materials have flawed IAS packing, and encompass deviations from ideal amorphous packing that give rise to local short and medium range arrangements of atoms. Short range order, limited to individual primary clusters, is likely to form during the cooling process if the interatomic interactions overcome the thermal fluctuations entropic effect. Medium range order may form during annealing by diffusion and atomic rearrangement, usually around the clusters with short range order. Density variations within the glass structure expedite this process. The latter process is similar to recrystallisation observed in heavily strained polycrystalline metals.

Short and medium range order means that the local arrangement of atoms in their immediate neighbourhood acquires either some geometrical symmetry elements or recurring chemical stoichiometry, or both. For as long as these remain below detectable levels, they will be referred to as flaws in the amorphous packing. However, above some specific critical volume fraction the presence of these arrangements will begin to affect the properties of the amorphous material, and in that case will be described as nano-crystals or nano-particles.

References

- Aste, T., Saadatfar, M., Sakellariou, A. and Senden, T.J. (2004) Investigating the geometrical structure of disordered sphere packings. *Physica A*, **339**, 16–23.
- Barlow, W. (1883) Probable nature of the internal symmetry of crystals. *Nature (London)*, **29** (738), 186–188.
- Bernal, J.D. (1959) A geometrical approach to the structure of liquids. *Nature*, **183** (4655), 141–147, doi: 10.1038/183141a0.
- Brostow, W., Dussault, J.-P. and Fox, B.L. (1978) Construction of voronoi polyhedra. *Journal of Computational Physics*, **29/1**, 81–92.
- Clare, B.W. and Kepert, D.L. (1986) The closest packing of equal circles on a sphere. *Proceedings of the Royal Society of London Series A: Mathematical and Physical Sciences*, **405** (1829), 329–344.
- Conway, J.N. and Sloane, N.J.A. (1998) *Sphere Packings, Lattices and Groups*, 3rd edn, Springer-Verlag, New York.
- Cottrell, A. (1965) *Dislocations and Plastic Flow in Crystals*, Clarendon Press, Oxford, New York.
- De-Floriani, I., Falcidieno, B. and Pienovi, C. (1985) Delaunay-based representation of surfaces defined over arbitrary shaped

- domains. *Graphics and Image Processes*, **32**, 127–140.
- Dirichlet, G.L. (1850) Über die Reduktion der Positiven Quadratischen Formen mit. Drei Unbestimmten Ganzen Zahlen. *Journal für die Reine und Angewandte Mathematik*, **40**, 216.
- Edwards, S.F. and Grinev, D.V. (2002) Granular materials: towards the statistical mechanics of jammed configurations. *Advances in Physics*, **51**, 1669–1684.
- Finney, J.L. (1970a) Random packings and the structure of simple liquids. i. the geometry of random close packing. *Proceedings of the Royal Society of London Series A: Mathematical and Physical Sciences*, **319** (1539), 479–493.
- Finney, J.L. (1970b) Random packings and the structure of simple liquids. ii. the molecular geometry of simple liquids. *Proceedings of the Royal Society of London Series A: Mathematical and Physical Sciences*, **319** (1539), 495–507.
- Flynn, C.P. (1972) *Point Defects and Diffusion*, Clarendon Press, Oxford.
- Furth, R. (1964) A new approach to the statistical thermodynamics of liquids. *Proc. R. Soc. Edinburgh*, **66**, 232.
- Hales, T.C. (1998) The Kepler conjecture. *arXiv preprint math/9811078*, <http://arxiv.org/abs/math/9811078> (accessed 25 June 2014).
- Haüy, R.J. (1821) *Traité Élémentaire De Physique*, Bachelier, Paris.
- Hoff, K.E., Culver, T., Keyser, J., Lin, M. and Manocha, D. (1999) Fast computation of generalised voronoi diagrams using graphics hardware. *SIGGRAPH99 Conference Proceedings*, ACM, p. 277.
- Kepler, J. (1611) *De Nive Sexangula*, Elsevier.
- Kopsias, N.P. and Theodorou, D.N. (1998) Elementary structural transitions in the amorphous lennard-jones solid using multidimensional transition-state theory. *Journal of Chemical Physics*, **109** (19), 8573–8582.
- Lee, Ch.-Y., Stachurski, Z.H. and Welberry, T.R. (2010) The geometry, topology and structure of amorphous solids. *Acta Materialia*, **58** (2), 615–625.
- Leopardi, P. (2006) Equally spaced points on a sphere. *Electronic Transactions on Numerical Analysis*, **25**, 309–327.
- Medvedev, N.N., Geiger, A. and Brostow, W. (1990) Distinguishing liquids from amorphous solids: percolation analysis on the voronoi network. *J. Chem. Phys.*, **93** (11), 8337–8342.
- Mott, P.H., Argon, A.S. and Suter, U.W. (1992) The atomic strain tensor. *Journal of Computational Physics*, **101**, 140.
- Pfister, L.A. and Stachurski, Z.H. (2002) Micromechanics of stress relaxation in amorphous glassy pmma part ii: application of the rt model. *Polymer*, **43**, 7419–7427.
- Reiss, H. and Hammerich, A.D. (1986) Hard spheres: scaled particle theory and exact relations on the existence and structure of the fluid/solid phase transition. *Journal of Physical Chemistry*, **90** (23):6252–6260, doi: 10.1021/j100281a037.
- Stachurski, Z.H. (2003) Definition and properties of ideal amorphous solids. *Physical Review Letters*, **90** (15), 5502–5506.
- Stachurski, Z.H. and Brostow, W. (2001) Methamorphosis of voronoi polyhedra as a definite measure of the elastico-dissipative atomic displacement transition. *Polimery*, **46** (5), 302–306.
- Tanemura, K. (1983) A new algorithm for three-dimensional voronoi a new algorithm for three-dimensional voronoi tessellation. *Journal of Computational Physics*, **51**, 191–207.
- Taylor, C.C.W. (1999) *The Atomists: Leucippus and Democritus*, University of Toronto Press.
- Theodorou, D.N. and Suter, U.W. (1985) Atomistic modelling of mechanical properties of polymeric glasses. *Macromolecules*, **19** (1) 379–387.
- To, L.Th., Daley, D.J. and Stachurski, Z.H. (2006) On the definition of an ideal amorphous solid. *Solid State Sciences*, **8**, 868–879.
- Torquato, S. (2002) *Random Heterogenous Materials*, Springer-Verlag, New York.
- Torquato, S., Truskett, T.M. and Debenedetti, P.G. (2000) Is random close packing of spheres well defined? *Physical Review Letters*, **84** (10), 2064–2067.
- Tsumuraya, K., Ishibashi, K. and Kusunoki, K. (1993) Statistics of voronoi polyhedra in a model silicon glass. *Physical Review B*, **47** (14), 8552–8557.

- Turek, I. (1997) *Electronic Structure of Disordered Alloys, Surfaces and Interfaces*, Kluwer Academic Publishers, Boston, MA.
- Voronoi, G. (1908) Recherches sur les paralléloedresprimitifs. *Journal für die reine und angewandte Mathematik*, **134**, 198–287.
- Voronoi, G. (1909) Nouvelles applications des paramètres continus à la théorie de formes quadratiques. *Journal für die reine und angewandte Mathematik*, **136**, 67.
- Walker, A.M., Slater, B., Gale, J.D. and Wright, K. (2004) Predicting the structure of screw dislocations in nanoporous materials. *Nature Materials*, **3** (10), 715–720.
- Watanabe, M.S. and Tsumaraya, K. (1987) Crystallisation and glass formation in liquid sodium: a molecular dynamics study. *Journal of Chemical Physics*, **87** (8), 4891.
- Wieder, T. and Fuess, H. (1997) A generalized debye scattering equation. *Zeitschrift für Naturforschung*, **52a**, 386–392.
- Wigner, E.P. and Seitz, F. (1933) On the constitution of metallic sodium. *Physical Review*, **43**, 804–810.
- Gittus, J. (1975) Creep, Viscoelasticity and Creep Fracture of Solids. *Appl. Sci. Publ.*, London.

A selected list of books on topics covered in this chapter.

Books on Crystallography

- Buerger, M.J. (1956) *Elementary Crystallography*, John Wiley & Sons, Inc., New York.
- Friedel, G. (1964) *Leçons de Crystallographie*, Blanchard, Paris.

Books on Glasses

- Doremus, R.H. (1973) *Glass Science*, John Wiley & Sons, Inc., New York.

Zarzycki, J. (1991) *Glasses and the Vitreous State*, Cambridge University Press, Cambridge.

Books on Random Walks

- Barber, M.N. and Ninham, B.W. (1970) *Random and Restricted Walks Theory and Application*, Gordon and Breach, New York.
- Hughes, B.D. (1995) *Random Walks and Random Environments*, Clarendon Press, Oxford.
- Rudnick, J. and Gaspari, G. (2004) *Elements of the Random Walk*, Cambridge University Press, Cambridge.

Books on Sphere Packings

- Conway, J.N. and Sloane, N.J.A. (1998) *Sphere Packings, Lattices and Groups*, 3rd edn, Springer-Verlag, New York.
- Daley, D.J. (2000) Packings and Approximate Packings of Spheres. Technical Report, National Institute for Statistical Sciences, grant No DMS- 9313013.
- Sadoc, J.-F. and Mosseri, R. (1999) *Geometrical Frustration*, Cambridge University Press, Cambridge.
- Zong, C.M. (1999) *Sphere Packings*, Springer-Verlag, New York, ISBN: 978-0-387-22780-1.

Books on Crystal Imperfections

- Flynn, C.P. (1972) *Point Defects and Diffusion*, Clarendon Press, Oxford.
- Kelly, A. and Groves, G.W. (1973) *Crystallography and Crystal Defects*, Longman, London.
- Nelson, D.R. (2002) *Defects and Geometry in Condensed Matter Physics*, Cambridge University Press.